Aichele, Martin; Crotti, Marco Giovanni; Rehle, Benedikt

Working Paper

A universal stress scenario approach for capitalising non-modellable risk factors under the FRTB

EBA Staff Paper Series, No. 14

Provided in Cooperation with:
European Banking Authority (EBA), Paris La Défense

Suggested Citation: Aichele, Martin; Crotti, Marco Giovanni; Rehle, Benedikt (2021) : A universal stress scenario approach for capitalising non-modellable risk factors under the FRTB, EBA Staff Paper Series, No. 14, ISBN 978-92-9245-747-1, European Banking Authority (EBA), Paris La Défense, https://doi.org/10.2853/859367

This Version is available at:
https://hdl.handle.net/10419/299519

EBA STAFF PAPER SERIES

N. 14 – JULY/2021

A UNIVERSAL STRESS SCENARIO APPROACH FOR CAPITALISING NON-MODELLABLE RISK FACTORS UNDER THE FRTB

by Martin Aichele, Marco Giovanni Crotti, and Benedikt Rehle

EBA EUROPEAN BANKING AUTHORITY

ABSTRACT

EU legislators mandated the European Banking Authority to propose a stress scenario methodology for capitalising non-modellable risk factors (NMRF) as foreseen under the Basel Fundamental Review of the Trading Book (FRTB) rules for market risk. In this paper, we present the foundations of such a methodology.

By design, it is universally applicable to all kinds of risk factors to which a bank may be exposed, and it caters for a wide range of data availability by adjusting the stress scenario for the number of returns observed in the calibration period. It captures non-linearities in the portfolio loss profile against changes in the NMRF, while reducing the computational effort and being simple.

To motivate the values set for some parameters in the methodology, we use a set of skewed generalised 't' (SGT) distributions as a generic tool for describing a wide universe of real historical returns from all asset classes.

Finally, we extend the methodology from single risk factors to segments of curves or surfaces as envisaged in the FRTB.

KEYWORDS

Market risk; FRTB; NMRF; capital requirements for non-modellable risk factors; sampling error for the expected shortfall; SGT distributions.

JEL CLASSIFICATION:

C13; C46; G21; G28; G32

1 Introduction

In January 2019, the Basel Commitee on Banking Supervision (BCBS) published the final revised global standard for banks' minimum capital requirements for market risk, also known as the Fundamental Review of the Trading Book (FRTB) [Bas19]. Under those standards, banks have the choice to use a so-called standardised approach based on sensitivities and prescribed "risk weights" or, subject to supervisory approval, to devise their own internal risk measurement model for computing capital requirements.

A key-feature of the FRTB is the classification of risk-factors that a bank has identified for their risk measurement as 'modellable' or 'non-modellable'. The risk-factor eligibility test (RFET) determines whether a risk factor is modellable or not. To be modellable, the number of 'real-price observations' observed over the last year needs to be at least 100 and be free of long streaks for no observations. Real price observations must be a real transaction or committed quote and be representative for the risk factor, i.e. the bank must be able to extract the value of the risk factor from the value of the real-price observations to use the observation for the RFET of that risk factor.

Modellable risk factors are capitalised in an integrated expected shortfall measure allowing for diversification and hedging among all modellable risk factors, with some restrictions for diversification across risk classes (general interest rates, credit spreads, equities, FX, and commodities). The ES measure is calibrated to a period of financial stress, i.e. a period that maximises the capital requirements for the bank's portfolio.

Non–modellable risk factors (NMRF) are capitalised, outside and incremental to the expected shortfall (ES) measure, under the 'stress scenario risk measure' (SSRM) which the FRTB does not specify in detail. Paragraph MAR 33.16 of the FRTB only states that it should be calibrated to be at least as prudent as the expected shortfall used for modelled risks (i.e. a loss calibrated to a 97.5% confidence level over a period of stress). It should be determined for each risk factor or, subject to supervisory approval, for each risk factor bucket (i.e. segments of a risk curve or surface). The risk factor (bucket) correlations are implicitly prescribed by an aggregation formula for the total capital requirement for non-modellable risk factors.

In May 2019, the European Parliament and Council adopted amendments to the Capital Requirements Regulation ([PC13, PC19]) implementing the FRTB standards in the European Union. In that context, the legislators mandated the European Banking Authority (EBA) to develop a methodology for determining the SSRM for capitalising NMRF. According to EU regulation an 'extreme scenario of future shock' must be determined for each non-modellable risk factor (bucket) that leads to a loss, which is the SSRM of that NMRF. In this paper, we present the design goals and mathematical foundations of the methodology that we designed to deliver on that mandate. Probably due to the FRTB novelties, and except for [MBP17], we are not aware of any prior work putting forward a methodology for capitalising NMRFs.

Banks could capitalise a non–modellable risk factor by direct historical simulation of losses per risk factor (bucket), which we call the 'direct method': first, the returns observed for the NMRF in a period of financial stress are obtained, then those returns are applied as shocks to the current value of the NMRF so as to obtain a sample of losses. The stress scenario risk measure would be the expected shortfall of the losses at 97.5% confidence level. However, the direct method requires a significant computational effort: for each risk factor (bucket) the losses of the portfolio positions susceptible to this risk factor would need to be calculated for each return in the stress period. This method is thus computationally very demanding for a trading book having potentially thousands of NMRFs and is not suited for risk factors with sparse data. Hence, there is a need for a much more efficient approach, which also has to be extendible to a low number of returns down to no observed returns at all in the stress period.

A recurrent underlying theme of this work is to consider the situation of less than daily returns for non-modellable risk factors, because NMRFs are typically less liquid and even more so in a stress period. However, it should be noted that there are in practice daily data for some non-modellable risk factors (i.e. daily risk factor returns can be computed), while the requirement to find real-price observations, so as to pass the RFET, is not met.

The paper is organised as follows. In Section 2, we outline the methodology by first introducing its design

goals and assumptions. We describe the concept of nearest to 10-(business) day returns scaled to 10 days catering for sparse data in the stress period, we put forward the 'asymmetrical sigma method', a method to obtain a robust approximation of the expected shortfall from a small sample of data, and we develop a computationally efficient approximation of the expected shortfall of the losses due to a risk factor by the loss corresponding to the expected shortfall of the risk factor distribution. In Section 3, we discuss corner cases under which the methodology may not lead to appropriate results and present ad-hoc solutions to address them. In Section 4, we show how to compensate for the small sample uncertainty in the estimation of the risk measures to a controlled target confidence level. In Section 5, we first give analytical expressions for Value-at-Risk (VaR) VaR and ES of the skewed-generalised t (SGT) distributions. We then use the SGT distributions as a tool for motivating the values taken by the parameters of our methodology, and in particular for investigating the small sample uncertainty of the ES estimates by means of a quantile approximation and Monte Carlo simulations. In Section 6, we show how the methodology is naturally extended to a bucket of risk factors in a curve or surface. In Section 7, we recall the final aggregated capital requirements for non-modellable risks and in Section 8, we conclude.

The building blocks of the methodology that are laid down in a detailed manner in this paper, namely, (i) a parsimonious way to obtain a time series of 10 days returns for risk factors with non-daily data; (ii) the asymmetrical sigma method ES estimator to robustly estimate ES measures on the basis of a volatility measure for small samples; (iii) the efficient approximation of the ES of losses with the loss at the ES of the risk factors' distribution by means of a non-linearity correction coefficient; (iv) the introduction of a sampling error compensation factor; and (v) the use, for calibration and analyses purposes, of a SGT distribution family broadly matching a large set of historically observed risk factors, are our main contributions. Linking all pieces together to obtain a universally applicable and efficient methodology for the SSRM that works also from a regulatory perspective can be considered our most relevant contribution. Finally, we believe that the analysis and results obtained for SGT distributions may also be useful in contexts other than the one discussed in this paper.

2 The methodology and the goals that drove its design

In this section we first introduce the goals that drove the design of the methodology and a few assumptions for it to be applied. We then present the methodology designed to overcome the drawbacks of a direct calculation of the expected shortfall of the losses while meeting those goals.

2.1 Goals and assumptions

The methodology is designed to meet the following goals:

- **G1**: Be applicable to any kind of risk factor. Typically banks' portfolios are susceptible to a vast range of risk factors that heavily differ in their nature: equity risk factors, interest rate risk factors, parameters used for modelling curves and surfaces. Thus, one of the goals of the methodology is its universal applicability.
- **G2**: Capture a wide range of different cases with respect to the number of observations available for a given risk factor. There may be risk factors for which banks have daily data, while for some others, the data availability is very limited. Thus, the methodology is designed to work with any data availability.
- **G3**: Ensure an adequate level of capitalisation for the non-modellable risk factors. In order to be in line with the FRTB standards, the methodology should lead to a stress scenario risk measure at least as prudent as the expected shortfall calibration used for modellable risk factors.
- **G4**: Be efficient and simple. The methodology should be efficient and use as few loss evaluations as possible without compromising other goals. It should be simple and remove complexity where possible.

- **G5**: Be applicable both at risk-factor level and at bucket level. The FRTB specifies that a stress scenario has to be generated for each NMRF separately. However, the FRTB also provides for the possibility to assess the modellability of risk factors belonging to a curve or a surface via either the own bucketing approach or the regulatory bucketing approach. Where a bank opts to use regulatory buckets, it can generate a stress scenario for all risk factors in the bucket, and determine the capitalisation at bucket level. Thus, the methodology must be designed to be applicable at bucket level as well.

- **G6**: Capture losses accurately. The methodology must accurately capture the characteristics of the loss functions with respect to movements in the risk factors.

- **G7**: Less data, more capital. The methodology should be built to obtain higher capital requirements when less data are available so as to reflect the uncertainty that is present when obtaining figures with few data.

When developing the methodology we assumed that:

- **A1**: When applying the methodology, banks have identified the portfolio the positions of which are capitalised in accordance with internal models approach - we refer to it as the 'SSRM portfolio'. Specifically, in accordance with the FRTB, only positions in trading desks meeting the backtesting and P&L attribution requirements can be capitalised by means of internal models.

- **A2**: When applying the methodology, banks have a fixed set of risk factors that passed the risk factor eligibility test and have been classified as modellable and a fixed set of risk factors that did not pass that test and have been classified as non–modellable.

- **A3**: For each of the five risk classes identified in the FRTB (e.g. equity risk), the bank identified a 12-month period of financial stress S – we refer to it as 'stress period' – for which a sufficient amount of data is available for calibrating shocks applicable to the NMRFs in the risk class. Paragraph 33.16 of the FRTB sets out that a common 12-month period of stress across all NMRFs in the same risk class must be used for obtaining the stress scenario risk measures. That prerequisite is at the basis of our assumption.

- **A4**: For each non–modellable risk factor j, banks can identify the loss that their SSRM portfolio would suffer following a change in the value of the NMRF. Equivalently, banks are able for each shock x to determine the corresponding portfolio's loss $l_j(x)$,

$$l_j(x) = \text{Loss}_{D^*}(r_j^* \oplus x)\,, \tag{1}$$

  where D^* denotes the date for which the stress scenario risk measure is calculated - we refer to it as 'reference date', r_j^* the value of the NMRF j at reference date, and $\oplus$ denotes the application of the shock x to the risk factor value r_j^* in accordance with the risk factor return modelling used (e.g. absolute returns, logarithmic returns, etc.)[1]. The loss function $\text{Loss}_{D^*}(r_j)$ is defined as follows:

$$\text{Loss}_{D^*}(r_j) = PV(r_j^*) - PV(r_j)\,, \tag{2}$$

  where $PV(r_j)$ denotes the present value of the portfolio as a function of r_j, the value of the NMRF j.

In the paper, we will flag important cases where a design choice has been made to fulfil one of the listed goals. We will also recall, where relevant, the assumptions made.

[1]The shock x can be either positive or negative. When a shock is positive, the operator $\oplus$ applies an upward shock to the risk factor. Vice versa when x is negative a downward shock is applied

2.2 The methodology

Having set the goals and laid down some basic assumptions, we are now ready to present the methodology to determine the stress scenario risk measure for a NMRF.

In accordance with paragraph MAR 33.12 of the FRTB, each risk factor in the bank's internal model is mapped to a specific liquidity horizon. Following the mapping, modellable risk factors are capitalised determining an expected shortfall measure calibrated on a 10-day horizon which is then rescaled to reflect the liquidity horizons of the modelled risks. To be consistent with the treatment envisaged for modellable risk factors, we reduce the problem of obtaining a stress scenario risk measure already capturing the risk factor liquidity horizon to the one of obtaining a stress scenario risk measure on a 10-day horizon, $SS_{10\mathrm{d}}$. Only at the final stage, we will rescale $SS_{10\mathrm{d}}$ to reflect the liquidity horizon of the non-modellable risk factor. Hence, the outcome of the methodology should be the identification of a loss under a stress scenario calibrated on a 10-day horizon.

To address the drawbacks resulting from a direct calculation of the expected shortfall of the losses, i.e. via the direct method presented in the introductory section, we propose in our methodology an approach based on the determination of the stress scenario risk measure $SS_{10\mathrm{d}}$ starting from the expected shortfall of the distribution of the 10-days returns observed for the NMRF in the stress period. Consistently with goal G3, such an approach should lead to:

$$SS_{10\mathrm{d}} \approx \mathrm{ES}(l(X), \alpha)\,, \tag{3}$$

having denoted with X the random 10-day return for the NMRF in the stress period, and $1-\alpha = 97.5\%$ being the confidence level of the ES measure.

We summarise the methodology as follows: first, we determine a time series of 10-business-day returns for the NMRF in the stress period and, from that time series, we estimate or approximate the left-tail and right-tail expected shortfall of the return distribution. Subsequently, we investigate the loss profile due to a change in the NMRF within the range identified by the two tail measures. Finally, we link that loss profile with the expected shortfall of the losses, so as to obtain a stress scenario risk measure that attracts a sufficient level of capital as in approximation in Eq. 3. As it will be clearer later, that link will mostly be based on the switch between the loss function operator $l(.)$ and the ES operator, i.e. we will link $\mathrm{ES}(l(X))$ with $l(\mathrm{ES}(X))$.

2.2.1 Building a time series of 10-business-day returns

For a risk factor with daily data, the determination of a time series of rolling 10-business-day returns is trivial as the identification of a 10-days-rolling period is always possible. However, as mentioned in goal G2, NMRF data may be sparse; hence, our methodology generalises the concept of a 10-business-day return to a 'nearest' to 10-business-day return to meet that goal. More specifically, we built up a parsimonious recipe based on the identification of the return on the nearest to 10-business-day window, that is then rescaled to obtain a return reflecting a 10-business-day period using the square-root-of-time rule employed in the FRTB for modellable risk factors.

Let $[D_1, D_2, ..., D_M]$ be the vector representing the dates within the stress period S for which an observation for the NMRF j is present, and let $[D_{M+1}, ..., D_{M+d-1}, D_{M+d}]$ be the vector representing the observation dates in the 20-business-day period following the stress period S. For each date index $t \in [1, 2, ..., M-1]$, we identify a "nearest next to 10 days" date index $t_{\mathrm{nn}}(t)$ by minimising the absolute relative deviation[2]:

$$t_{\mathrm{nn}}(t) = \underset{t'>t,\ t'\in[2,\ldots,M+d]}{\operatorname{argmax}} \left| \frac{10 \text{ days}}{D_{t'} - D_t} - 1 \right| . \tag{4}$$

Once $t_{\mathrm{nn}}(t)$ is determined, the return on the period identified by the two dates D_t and $D_{t_{\mathrm{nn}}(t)}$ is computed. The date index $t \in [1, \ldots, M-1]$, indexing the 'starting observation' used to determine a return, corresponds always to a date in the 1-year stress period, while $t' \in [2, \ldots, M, M+1, \ldots M+d]$ might correspond to an 'ending

[2] As a rare special case, where an observation at both the 6th and 30th business days forward date $D_{t'}$ is available, with no dates in between (i.e. they both minimise the relative deviation), t' corresponding to the observation that occurred 30 business days after D_t is to be selected as $t_{\mathrm{nn}}(t)$.

Figure 1: This figure shows a flow-chart of the various steps that banks are to perform to capitalise their risk factors (RF) according to the currently proposed EU technical standards. First, banks assess with the risk-factor eligibility test (RFET) whether a RF is modellable or not. Then, the nearest to 10-day returns are computed. For the non-modellable RF the green box groups the steps of the methodology described in this paper. Depending on the number of returns in the one year stress period, different estimation methods are used to calibrate shocks to the left and right ES(97.5%). To cater for different signs of the sensitivity to the shocks (long or short) the highest loss occurring in the range from down to up shock is taken as the stress scenario risk measure basis value. Corrections for non-linearity, estimation uncertainty and a rescaling to the applicable liquidity horizon are applied as needed. For completeness we also include the 'direct method', i.e. where banks compute the losses when shocking the portfolio by the 10-day returns in the stress period from which the expected shortfall of those losses is used directly as stress scenario risk measure on a 10-day horizon. That method can be used only where the number of returns available ensure a robust ES estimation as in the historical method presented in this paper, [EBA20b] limits its use to cases where $N \geq 200$.

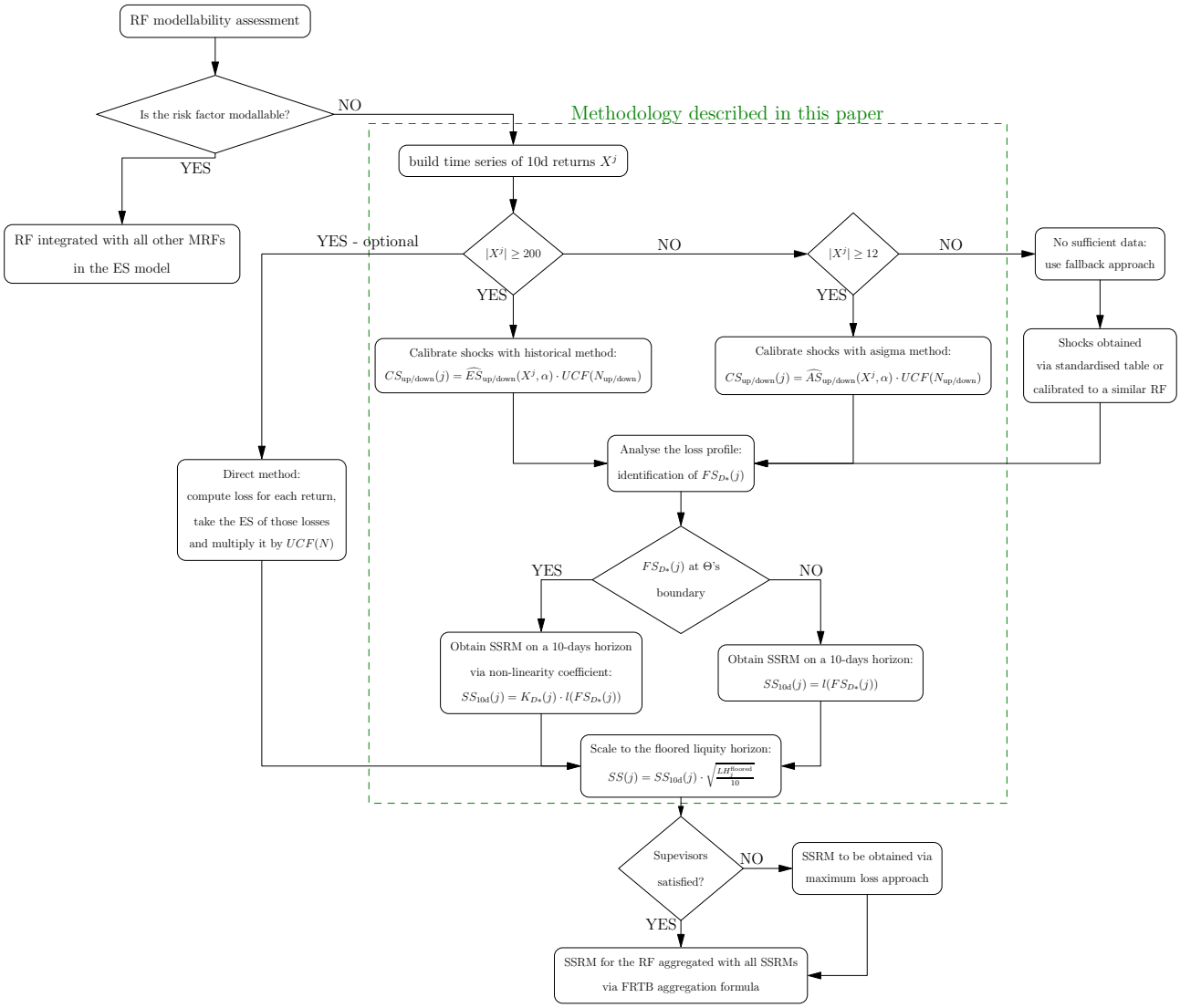

observation' date in the 20-business-day period following the stress period. We extended the stress period S with 20 business days so as to avoid that too many returns at the end of S are obtained using the observation at D_M - potentially leading the last observation in S to be overly represented. The return on the period identified by the two dates D_t and $D_{t_{\mathrm{nn}}(t)}$, is finally rescaled by $\sqrt{\frac{10 \text{ days}}{D_{t_{\mathrm{nn}}(t)} - D_t}}$ to get a return on a 10-business-day period. Eq. 4 for $t_{\mathrm{nn}}(t)$ privileges the rescaling of a longer-than-10-day return to a 10-day return over the rescaling of a shorter-than-10-day return to a 10-day return if compared to a formula that identifies $t_{\mathrm{nn}}(t)$ by minimising $|D_{t'} - D_t - 10 \text{ days}|$ or $\left|\sqrt{\frac{10 \text{ days}}{D_{t'} - D_t}} - 1\right|$. In particular, dates distancing from D_t for more than 10 business days are always preferred to dates distancing for 5 or fewer business days. Favouring longer-dated returns was done considering that paragraph MAR 33.16 of the FRTB sets out that the liquidity horizon of a NMRF must be greater than or equal to 20 days – thus, longer horizons will likely be closer to the final applicable liquidity horizon. In addition, rescaling shorter returns to a longer period brings with itself the possibility of amplifying short term movements; vice versa, rescaling longer returns to a shorter period tends to remove those short term effects.

Other methods for constructing a 10-business-day returns time-series by imputation of data in case of missing observations could be envisaged. However, they might require a time-series modelling (e.g. via a GARCH model approach) and might need a fitting or regression procedure. This would increase complexity, in contrast to Goal G4, and different kinds of risk factors might require different approaches, in contrast to Goal G1.

As a result, regardless of the amount of NMRF observations in the stress period, a time series with $N = M-1$ returns is obtained. We denote with X^j, the sample of returns for the NMRF j in the time series obtained as a result of this step. From that sample, our objective is to obtain two shocks resembling the right and left-tail expected shortfall of the return distribution, with the idea of linking them with the expected shortfall of the losses calculated on that return distribution (i.e. linking ES(X) with ES($l(X)$).

2.2.2 Calibrating extreme shocks from the sample X^j

As mentioned, we now want to calibrate an upward and downward shock for the NMRF j, respectively $CS_{\mathrm{up}}(j)$ and $CS_{\mathrm{down}}(j)$, from the sample of returns X^j. The two calibrated shocks are estimates of the right-tail and left-tail expected shortfall of the distribution of the 10-business-day returns for the NMRF j in the stress period.

In goal G2, we stated that processing for a wide of range of cases with respect to number of returns available in the stress period should be possible. An α-tail ES estimation from a large sample of N returns of which $[\alpha N]$ fall in the α-tail is not posing any problem. Having at least 5 observations in the tail, i.e. $N \geq 200$, leads to a sufficiently robust estimation, as we will show in Section 5.2.2. As a result, for calibrating $CS_{\mathrm{up}}(j)$ and $CS_{\mathrm{down}}(j)$, a historical estimator is used when at least $N^{\mathrm{hist}} = 200$ 10-day returns are available in the sample of returns X^j. $CS_{\mathrm{up}}(j)$ and $CS_{\mathrm{down}}(j)$ as determined by this 'historical method' are:

$$CS_{\mathrm{down}}(j) = \widehat{ES}_{\mathrm{down}}(X^j, \alpha) \cdot UCF(N) \tag{5}$$

and:

$$CS_{\mathrm{up}}(j) = \widehat{ES}_{\mathrm{up}}(X^j, \alpha) \cdot UCF(N)\,, \tag{6}$$

where $\widehat{ES}_{\mathrm{down}}(X^j, \alpha)$ and $\widehat{ES}_{\mathrm{up}}(X^j, \alpha)$ denote respectively the left α-tail and right α-tail historical expected shortfall estimators introduced in Eq. 7 or 8 applied to the sample X^j of returns for the NMRF j, and $\alpha = 2.5\%$. $UCF(N)$ is the uncertainty compensation factor for N returns to be introduced in Section 4 – it implements the principle introduced in G7 that less data should lead to more capital, and reflects the error in estimating the expected shortfall.

The following historical estimator for the expected shortfall for the left tail of the sample distribution is used:

$$\widehat{ES}_{\mathrm{down}}(X^j, \alpha) = \frac{-1}{\alpha N} \left\{ \sum_{i=1}^{[\alpha N]} X^j_{(i)} + (\alpha N - [\alpha N])\, X^j_{([\alpha N]+1)} \right\}, \tag{7}$$

where $X^j_{(i)}$ is the order statistics of the sample X^j of size N, and $[\alpha N]$ denotes the integer part of the product αN. We adopt a sign convention leading to a positive number for the left (negative) tail of a distribution centred

around zero like in [AT02]. This estimator (Eq. 23 in [NZC14]) is slightly different from the simple historical estimator which uses only the $[\alpha N]$ worst losses. It is more natural for the expected shortfall being an α-tail mean (cf. Definition 2.6 in [AT02]), accounts for αN not being an integer and is somewhat more stable by incorporating $X^j_{([\alpha N]+1)}$. The historical estimator for the α ES of the right tail is:

$$\widehat{ES}_{\text{up}}(X^j, \alpha) = \widehat{ES}_{\text{down}}(-X^j, \alpha)\,. \tag{8}$$

The sign convention is also leading to a positive number for the right (positive) tail of a distribution centered around zero. The estimators deliberately do not remove a mean (drift) in the return sample which is kept as a feature of return shocks in a stress period. While such a 'de-meaning' could be appropriate e.g. for FX rates and short liquidity horizons, where a zero-mean assumption might be warranted, we note that the risk factors are varied as stated in goal G1 and could e.g. also be parameters of a yield curve or volatility surface where a zero mean assumption would not apply. Furthermore, such 'de-meaning' would fit more for pricing purposes rather than for the purpose of generating risk measures calibrated to a stress period, i.e. based on historically observed data. That said, typically the means are small compared to the volatility or the ES.

If the number of returns N in the sample X^j is lower than N^{hist}, the robust estimation of the ES becomes more challenging. The key idea in our methodology for this case is to approximate the expected shortfall by rescaling a volatility measure, because the standard deviation can be estimated more robustly for a small sample than the ES with the historical estimator. The HÜRLIMANN bound [Hür02] states $\text{ES}(\alpha) \leq \mu + \sqrt{\frac{1-\alpha}{\alpha}}\sigma$ for any continuous distribution on $\mathbb{R}$ with given mean μ and standard deviation σ and motivates that the ES can be approximated by a (distribution dependent) multiple of σ when the mean is negligible. We will recover this location-scale dependency explicitly for the SGT distribution family in Subsection 5.1.

Instead of rescaling the standard deviation on the sample comprising all returns in the time series, our methodology splits the set of returns at the median into two halves, and on each half, a quantity resembling the mean and standard deviation is estimated. This allows for capturing asymmetry in a distribution which is often found in risk factor returns [EBA20a]. Higher than second moments are deliberately not used so as to make the estimator more robust against outliers and more suitable for small samples. Finally, to ensure that the standard deviations on the two halves are robustly estimated, the determination of $CS_{\text{down}}(j)$ and $CS_{\text{up}}(j)$ via such rescaling is limited to cases where there are at least $N \geq N^{\text{asigma}} = 12$ returns in the sample X^j – we motivate the value set for N^{asigma} in Subsection 5.2.2.

Formally, we first define the sets of returns in each half, $X^j_{\text{down}} := \{X^j \leq \text{med}(X^j)\}$ and $X^j_{\text{up}} := \{X^j > \text{med}(X^j)\}$ with $\text{med}(X^j)$ denoting the median of the sample of returns X^j and N_{down}, N_{up}, the cardinalities of the two sets. The calibrated shocks of this 'asymmetrical sigma' method are:

$$CS_{\text{down}}(j) = \widehat{AS}_{\text{down}}(X^j) \cdot UCF(N_{\text{down}}) \tag{9}$$

and

$$CS_{\text{up}}(j) = \widehat{AS}_{\text{up}}(X^j) \cdot UCF(N_{\text{up}})\,, \tag{10}$$

where $UCF(N_{\text{down}})$ and $UCF(N_{\text{up}})$ capture the uncertainty in approximating the expected shortfall measures, and where $\widehat{AS}_{\text{down}}(X^j)$ and $\widehat{AS}_{\text{up}}(X^j)$ are the 'asigma' estimators approximating the left and right tail expected shortfalls from the set X^j:

$$\widehat{AS}_{\text{down}} = -\widehat{\mu}_{X^j_{\text{down}}} + \frac{C^{\text{asigma}}_{\text{ES}}}{\sqrt{N_{\text{down}} - \frac{3}{2}}} \sqrt{\sum_{X^j_i \in X^j_{\text{down}}} \left(X^j_i - \widehat{\mu}_{X^j_{\text{down}}}\right)^2} = -\widehat{\mu}_{X^j_{\text{down}}} + C^{\text{asigma}}_{\text{ES}}\, \widehat{\sigma}_{X^j_{\text{down}}}\,, \tag{11}$$

where $\widehat{\mu}_{X^j_{\text{down}}}$ and $\widehat{\sigma}_{X^j_{\text{down}}}$ denote the mean and standard deviation estimators of the returns below the median. The minus sign in front of $\widehat{\mu}_{X^j_{\text{down}}}$ leads to a positive calibrated shock for the typical case that $\widehat{\mu}_{X^j_{\text{down}}} < 0$ when the median is near zero.

Analogously,

$$\widehat{AS}_{\text{up}} = \widehat{\mu}_{X^j_{\text{up}}} + \frac{C^{\text{asigma}}_{\text{ES}}}{\sqrt{N_{\text{up}} - \frac{3}{2}}} \sqrt{\sum_{X^j_i \in X^j_{\text{down}}} \left(X^j_i - \widehat{\mu}_{X^j_{\text{up}}}\right)^2} = \widehat{\mu}_{X^j_{\text{up}}} + C^{\text{asigma}}_{\text{ES}}\, \widehat{\sigma}_{X^j_{\text{down}}}\,. \tag{12}$$

The two estimators rescale estimates of the standard deviation on the two sets by $C_{\mathrm{ES}}^{\mathrm{asigma}}$. For small sample sizes, taking the square root of the usual sample estimator for the variance as the estimator for the standard deviation leads to a biased estimate due to JENSEN's inequality [Jen06, Ben03] and the convexity of the square root function. We use the approximately unbiased sample estimator for the standard deviation [GT71], keeping only the leading term $N-1.5$. Setting the constant $C_{\mathrm{ES}}^{\mathrm{asigma}}$ so as to ensure an approximation of the ES measure that leads to an adequate level of capitalisation of NMRFs as laid down in goal G3 is key. We set it to 3 for all risk factors - in Section 5, we motivate in detail our choice which was also confirmed by a calibration on a large collection of risk factors' historical data [EBA20a].

We have covered $N \geq 200$ with the historical method and $N \geq 12$ with the asymmetrical sigma method. Below $N^{\mathrm{asigma}} = 12$ returns, there are insufficient data to robustly approximate an ES with reasonable accuracy. In this case, Assumption A3 is considered to not be met in practice, hence, we do not address it in this section. However, we will briefly discuss this case in Section 7 where a fallback method is sketched.

As a result, for any N, the methodology yields a downward shock $CS_{\mathrm{down}}(j)$ and an upward shock $CS_{\mathrm{up}}(j)$. The large upward and downward shock span the shock range $[-CS_{\mathrm{down}}(j), CS_{\mathrm{up}}(j)]$. We now aim to identify the shock from this interval which leads to the highest portfolio loss in order to have a sufficient understanding of the loss profile to infer information about $\mathrm{ES}(l(x))$ – in particular, we are chiefly interested to determine whether the worst loss in the range occurs at its boundaries. This shock will be called the extreme scenario of future shock $FS_{D*}(j)$.

2.2.3 Analysing the loss profile in the range $[-CS_{\mathrm{down}}(j), CS_{\mathrm{up}}(j)]$

The loss function $l_j(x)$ describes the loss of a whole SSRM portfolio under variation of the single risk factor j. In the most typical situation, $l_j(x)$ is not available in analytical form and no shape properties, e.g. neither monotonicity nor extremal values, are known a priori. Therefore, the only way to understand the loss profile is to explicitly calculate $l_j(x)$ for various shocks x.

A natural and simple approach to finding the highest loss is to cover the range $[-CS_{\mathrm{down}}(j), CS_{\mathrm{up}}(j)]$ with a finite grid of points, evaluate $l_j(x)$ for every vertex and pick the largest value. Clearly, the finer the grid is chosen, the more precisely the maximum can be determined. However, each calculation of $l_j(x)$ amounts to a portfolio revaluation, which is computationally costly given that in that portfolio many instruments dependent on the NMRF j may be present. Moreover, the procedure has to be repeated for each NMRF and computation results cannot be reused over several reference dates as every change in the portfolio composition potentially changes the loss profiles with respect to all NMRFs. Scanning the shock range with a very granular grid would therefore entail a very large overall computational cost, in conflict with goal G4.

As a pragmatic solution, the methodology requires the evaluation of $l_j(x)$ on a grid Θ of only four points, comprising the two boundary and two inner points:

$$\Theta = \underbrace{\{-CS_{\mathrm{down}}(j), CS_{\mathrm{up}}(j)\}}_{\text{boundary points}} \cup \underbrace{\{-0.8\,CS_{\mathrm{down}}(j), 0.8\,CS_{\mathrm{up}}(j)\}}_{\text{inner points}} . \tag{13}$$

The extreme scenario of future shock $FS_{D*}(j)$ is given by the shock that leads to the highest portfolio loss:

$$FS_{D*}(j) = \operatorname*{argmax}_{x \in \Theta} l_j(x) . \tag{14}$$

With such a coarse-grained scanning grid, the methodology cannot be expected to identify the highest loss in the range under all circumstances. Importantly, though, it yields the correct outcome in the most common case. When the portfolio has a directional exposure to the NMRF j and hence $l_j(x)$ is monotonic, the worst loss in the range occurs for one of the boundary points. Concretely, for a net long position in j, the methodology correctly identifies $-CS_{\mathrm{down}}(j)$, for a net short position, it yields $CS_{\mathrm{up}}(j)$. Adding the loss evaluations at the 80% grid points makes the methodology more robust when extreme tail hedges are in place[3]. In theory, $l_j(x)$

[3]The choice of including the point $0.8\,CS_{\mathrm{up}}(j)$ was also done with a view to the non-linearity correction introduced in Subsection 2.2.4 and is further motivated in 5.2.3

can be an arbitrarily complicated function with maxima well inside the interval, which will not be picked up by the methodology. However, given that portfolios tend to be fairly well hedged against small risk factor fluctuations, focusing exclusively on large returns yields adequate results in most practical cases [EBA20a] – hence, our choice to limit the loss evaluation to those four points only.

Consistently with goal G3, the methodology aims at estimating the expected shortfall of losses. We therefore have to link the loss $l_j(FS_{D*}(j))$ to $\mathrm{ES}(l_j(X))$. By definition, the expected shortfall is the average of the worst 2.5% losses and hence depends on both the return distribution and the shape of the loss function $l_j(x)$ in a potentially non-trivial manner[4]. As said, we cannot use detailed information on $l_j(x)$ as this would increase the computational footprint. Instead, we rely on further assumptions, dependent on whether the scenario corresponds to a shock from the inside or the boundary of the shock range. For the time being, let us assume that at least one of the four points from Θ actually leads to a loss so that $l_j(FS_{D*}(j)) > 0$. We distinguish the case where $FS_{D*}(j)$ is at the boundaries of Θ from the case where it is in the inner point. We will briefly discuss corner cases, e.g. cases where $l_j(FS_{D*}(j)) \leq 0$, in Section 3.

2.2.4 Obtaining $SS_{10\mathrm{d}}$ when $FS_{D*}(j)$ is at the boundaries of Θ via a non-linearity correction

We expect in the vast majority of cases the extreme scenario of future shock $FS_{D*}(j)$ to be at the boundaries of Θ, given that trading portfolios tend to be fairly well hedged against small risk factor fluctuations, and that, typically, for large shocks – like those included in Θ – the losses are monotonic.

Therefore, where $FS_{D*}(j)$ is at the boundaries of Θ, we assume that the worst 2.5% losses are due to tail events of the return distribution. Concretely, where $CS_{\mathrm{up}}(j)$ leads to the highest loss, we assume that the 2.5% worst losses come from the 2.5% largest returns. Analogously, where the highest loss is associated with $-CS_{\mathrm{down}}(j)$, we assume that the 2.5% worst losses come from the 2.5% smallest (or most negative) returns. As part of a data collection exercise [EBA19], data on portfolio loss functions upon change in single risk factors were collected both for standardised portfolios (the EBA Supervisory benchmarking exercise portfolios [EBA21]) and some banks' real trading portfolios which included also structured products. Those data backed the presumption that banks portfolios are in general directional, i.e. that in the vast majority of cases the extreme shocks will be at the boundaries of Θ, and that the losses are in general monotonic for large shocks.

We formally investigate the case where $CS_{\mathrm{up}}(j)$ is the extreme scenario of future shock. The analysis for $-CS_{\mathrm{down}}(j)$ is fully analogous and differs only in signs. In Figure 2, we show the various elements that are discussed in this subsection.

Let $q_{97.5\%}(l_j(X))$ and $q_{97.5\%}(X)$ denote the 97.5th percentile of the loss and the return distribution, respectively. As stated above, we assume that $\{x|l_j(x) > q_{97.5\%}(l_j(X))\} = \{x|x > q_{97.5\%}(X)\}$. Using the equality of these two sets, the expected shortfall of losses can be calculated as

$$\mathrm{ES}(l_j(X)) = \frac{1}{2.5\%}\mathbb{E}\left(l_j(X) \cdot I_{X>q_{97.5\%}(X)}\right) , \tag{15}$$

where $I_{(\cdot)}$ denotes the indicator function. In other words, the expected shortfall is the average loss over tail events of X. To make this explicit, let X_{T} be a new random variable, distributed like X but conditional on X being larger than $q_{97.5\%}(X)$, i.e. $X_{\mathrm{T}} := X \cdot I_{X>q_{97.5\%}(X)}$. Note that $\mathbb{E}(X_{\mathrm{T}}) = \mathrm{ES}(X)$ by definition of the expected shortfall of X. We have:

$$\mathrm{ES}(l_j(X)) = \mathbb{E}(l_j(X_{\mathrm{T}})) . \tag{16}$$

If $l_j(x)$ was a linear function one could exchange it with the integral to find the equality $\mathrm{ES}(l_j(X)) = l_j(\mathrm{ES}(X))$. However, depending on whether $l_j(x)$ is convex or concave, Jensen's inequality for expected values [Jen06, Ben03] applies and the left-hand side can be significantly larger or smaller than the right-hand side, respectively. We capture this non-linearity effect by an analytical approximation.

[4]Different from our definition, the mathematics literature typically defines expected shortfall as an average of quantiles. However, the two definitions are equivalent for continuous distributions and hence for all practical purposes. Moreover, our definition coincides with the one given in paragraph MAR 10.18 of the FRTB.

To this end, we use a second-order Taylor expansion of $l_j(x)$ around $\mathrm{ES}(X)$:

$$\mathbb{E}\left(l_j(X_\mathrm{T})\right) = \mathbb{E}\left(l_j(\mathrm{ES}(X)) + \left.\frac{\partial l_j}{\partial x}\right|_{x=\mathrm{ES}(X)} (X_\mathrm{T} - \mathrm{ES}(X)) + \frac{1}{2}\left.\frac{\partial^2 l_j}{\partial x^2}\right|_{x=\mathrm{ES}(X)} (X_\mathrm{T} - \mathrm{ES}(X))^2\right) \tag{17}$$

and by noting that $\mathbb{E}(X_\mathrm{T}) = \mathrm{ES}(X)$, the linear term drops out from Eq. 17 and we find:

$$\mathbb{E}\left(l_j(X_\mathrm{T})\right) \approx l_j(\mathrm{ES}(X)) + \frac{1}{2}\left.\frac{\partial^2 l_j}{\partial x^2}\right|_{x=\mathrm{ES}(X)} \left(\mathbb{E}\left(X_\mathrm{T}^2\right) - \mathrm{ES}(X)^2\right) . \tag{18}$$

After reorganising terms and going back from X_T to X, the approximate expected shortfall of losses can be written as

$$\mathrm{ES}(l_j(X)) \approx l_j(\mathrm{ES}(X)) + \frac{1}{2}\Gamma\left(\phi - 1\right)\mathrm{ES}(X)^2 = l_j(\mathrm{ES}(X)) \cdot K\,, \tag{19}$$

where we have introduced the quantities

$$\Gamma := \left.\frac{\partial^2 l_j}{\partial x^2}\right|_{x=\mathrm{ES}(X)}\,, \quad \phi := \frac{\mathbb{E}\left(X_\mathrm{T}^2\right)}{\mathrm{ES}(X)^2} = \frac{\mathbb{E}\left(X^2 \cdot I_{X>q_{97.5\%}(X)}\right)}{\mathbb{E}\left(X \cdot I_{X>q_{97.5\%}(X)}\right)^2} \geq 1\,, \tag{20}$$

remembering that $\mathrm{ES}(X) = \mathbb{E}(X_\mathrm{T})$. The fact that $\phi \geq 1$ can be proved by applying Jensen's inequality with the convex function $f(x) = x^2$. With those quantities we define

$$K := 1 + \frac{1}{2}\frac{\Gamma}{l_j\left(\mathrm{ES}(X)\right)}\left(\phi - 1\right)\mathrm{ES}(X)^2\,. \tag{21}$$

This is our analytical approximation and we call K the 'non-linearity correction'. The formula for K nicely disentangles the two components that drive $\mathrm{ES}(l_j(X))$: Γ, the curvature of the loss function, and ϕ, which is a tail shape measure for how heavy the tails of the return distribution are. Both super-linear loss profiles and heavy-tailed return distributions are common features in financial markets, so arguably such non-linearity corrections can be non-negligible for real-world portfolios.

While the Taylor polynomial is a *local* approximation of $l_j(x)$ around $\mathrm{ES}(X)$, we use it as an approximation of $l_j(x)$ for all $x > q_{97.5\%}(X)$. The quality of the approximation can therefore vary substantially, depending on the global shape of $l_j(x)$. Later in this section we account for this by capping and flooring the non-linearity correction leading to Eq. 26.

Γ is the second derivative of $l_j(x)$ with respect to the return x around $\mathrm{ES}(X)$. We note that it can be non-zero even for portfolios consisting exclusively of linear products in the risk factor. This is the case when returns are applied non-linearly to a risk factor, i.e. when $r_j^* \oplus x$ is a non-linear function of x. The typical example are log returns for which $l_j(x) = \mathrm{Loss}_{D*}(r_j^* \oplus x) = \mathrm{Loss}_{D*}(r_j^* \cdot e^x)$.

We determine the derivative numerically using a second-order finite central differences formula [Far93]. Setting $h = 0.2\,\mathrm{ES}(X)$, we have:

$$\Gamma \approx \frac{l_j\left(\mathrm{ES}(X) - h\right) - 2\,l_j\left(\mathrm{ES}(X)\right) + l_j\left(\mathrm{ES}(X) + h\right)}{h^2}\,. \tag{22}$$

The relatively large step width parameter h limits the dependence on local peculiarities of $l_j(x)$ around $\mathrm{ES}(X)$. Instead, the derivative based on these three points can rather be thought of as a global indicator of the curvature of $l_j(x)$ in the tail regime for the purpose of integration from $\mathrm{VaR}(X)$ to ∞. In Section 5.2.3 we motivate the value for h by showing that for a wide range of risk factors, $q_{97.5\%}(X) = \mathrm{VaR}(X, 97.5\%) \approx \frac{4}{5}\mathrm{ES}(X, 97.5\%)$, so that $h = 0.2$ means to take the inner point of the Γ computation approximately as the lower bound of the integration for the non-linearity correction.

An alternative interpretation is the following: rather than replacing the loss profile by the tangential Taylor parabola, we effectively replace $l_j(x)$ by the single parabola that goes through the three points defining the derivative. To see this, note that linear terms drop out in the calculation above so that one can, without changing the result, tilt the Taylor parabola around $\mathrm{ES}(X)$ until it hits all three points.

The quantity ϕ characterises the heaviness of the tails of the return distribution, i.e. the dispersion of the returns in the tail around the ES value. Being a tail property, a sufficiently large sample of returns is required

to estimate ϕ. Where we have recorded at least $N \geq N_{\text{hist}} = 200$ returns, we determine ϕ using the statistical estimator $\widehat{ES}_{\text{up}}(X^j, \alpha)$ introduced in Eq. 8 combined with Eq. 20. We define the following estimator:

$$\widehat{\phi}_{\text{up}}(X^j, \alpha) = \frac{\frac{1}{\alpha N}\left\{\sum_{i=1}[\alpha N](-X^j)^2_{(i)} + (\alpha N - [\alpha N])\,(-X^j)^2_{([\alpha N]+1)}\right\}}{\widehat{ES}^2_{\text{up}}(X^j, \alpha)}\,. \tag{23}$$

where as in Eq. 7, the index (i) is used to indicate the order statistics. If less than $N^{\text{hist}} = 200$ returns are available, we do not rely on an estimator - hence, where the asigma method is used to determine the calibrated shocks, we use a flat value of $\phi^{\text{asigma}} = 1.04$. In Section 5.2.1 we motivate this constant which corresponds to the assumption that the return distribution has moderately heavy tails and was also confirmed by historical data [EBA20a].

We now combine these components to arrive at a concrete formula for the non-linearity correction coefficient $K_{D*}(j)$. Where the scenario of future shock is associated with $-CS_{\text{down}}(j)$, all occurrences of the right-tail expected shortfall $\text{ES}(X)$ have to be replaced by its left-tail counterpart. Moreover, the calculations in ϕ must refer to the left rather than the right tail of the distribution of X. Overall, we obtain:

$$\tilde{K}_{D*}(j) = 1 + \frac{25}{2}\,\frac{l_j(0.8\,FS_{D*}(j)) - 2\,l_j(FS_{D*}(j)) + l_j(1.2\,FS_{D*}(j))}{l_j(FS_{D*}(j))}\,\left(\widehat{\phi} - 1\right)\,, \tag{24}$$

where we set $\text{ES}(X)$ equal to $FS_{D*}(j)$ in Eqs. 20 and 22 given that the latter is the estimation or approximation of the former, and where:

$$\widehat{\phi} = \begin{cases} \widehat{\phi}_{\text{up}} & \text{if} \quad N \geq N_{\text{hist}} \text{ and } FS_{D*}(j) = CS_{\text{up}}(j); \\ \widehat{\phi}_{\text{down}} = \widehat{\phi}_{\text{up}}(-X^j, \alpha) & \text{if} \quad N \geq N_{\text{hist}} \text{ and } FS_{D*}(j) = -CS_{\text{down}}(j); \\ \phi^{\text{asigma}} = 1.04 & \text{if} \quad 12 \leq N < N_{\text{hist}}. \end{cases} \tag{25}$$

Finally, we apply a cap and a floor,

$$K_{D*}(j) = \max\left(K_{\min}, \min\left(\tilde{K}_{D*}(j), K_{\max}\right)\right)\,, \tag{26}$$

where $K_{\min} = 0.9$ and $K_{\max} = 5$. The floor at $K_{\min}$ limits unintended consequences of our approximation approach when the second derivative Γ at $FS_{D*}(j)$ is negative. Typically, this is indicative of a flattening loss profile for large returns, which justifies $K_{D*}(j) < 1$. However, recall that in this case, our methodology replaces the loss function $l_j(x)$ with a downward opening parabola. That is, the approximate loss profile does not only flatten, but actually bends and eventually turns negative (i.e. turns from losses into gains) for very large returns, which is highly unrealistic. It can be shown that under optimistic assumptions a maximum benefit of $K_{D*}(j) = 0.9$ can be expected; this can be seen by considering a hypothetical loss profile that grows linearly from zero, reaches the value $l_j(\text{ES}(X))$ at $x = \text{ES}(X)$ and then stays constant for all larger returns, which serves as our optimistic benchmark (cf. Figure 2). Γ can be calculated explicitly, and using $\phi = \phi^{\text{asigma}} = 1.04$ we find that $K_{D*}(j) = 0.9$ in this case. Therefore, where the formula for $K_{D*}(j)$ yields values smaller than 0.9, this is considered a relic of the approximation and the floor applies. The large cap at $K_{\max}$ corresponds to a very steep loss profile and is merely a precaution to prevent implausibly large results that could be triggered e.g. by numerical issues in approximating the second order derivative.

We also note that for $0.8\,FS_{D*}(j)$, we have already evaluated the loss function when searching the highest loss in Θ. Hence, in line with goal G4, only one additional loss function evaluation at $1.2\,FS_{D*}(j)$ is necessary to calculate $\tilde{K}_{D*}(j)$.

This marks the end of our discussion and we can finally calculate the 10-day SSRM for the case where the scenario of future shock is one of the boundary points of the shock range:

$$SS_{10\text{d}}(j) = K_{D*}(j) \cdot l(FS_{D*}(j)) \quad \text{if} \quad FS_{D*}(j) \in \{-CS_{\text{down}}(j); CS_{\text{up}}(j)\}\,. \tag{27}$$

As part of the data collection exercise [EBA19], the stress scenario risk measures resulting from the application of our methodology were provided. In a few cases, banks even reported the stress scenario risk measure

Figure 2: We show in an example how the worst loss is determined for a loss profile and the computation of the non-linearity correction $K_{D*}(j)$. The risk factor values of the grid Θ for which the loss must be evaluated are indicated on the x-axis. With the continuous red line, we depict the loss profile. In this example, the worst loss in the grid Θ occurs at CS_{up}. Hence, CS_{up} is the extreme scenario of future shock $FS_{D*}(j)$. The three points to calculate the non-linearity coefficient $K_{D*}(j)$ are identified with a red circle on the loss profile. We derived the parabola passing through the three points in the return space, and applied the operator $\oplus$ to that parabola, obtaining the corresponding curve in the risk factor space represented with a dotted red line. We also obtained a numerical value for the non-linearity correction $K_{D*}(j) = 1.33$ for the represented loss function assuming $\phi^{\text{asigma}} = 1.04$. Assuming $\phi^{\text{asigma}} = 1.04$, we also show with a purple dashed line a loss profile that would lead to reaching floor 0.9 for $K_{D*}(j)$.

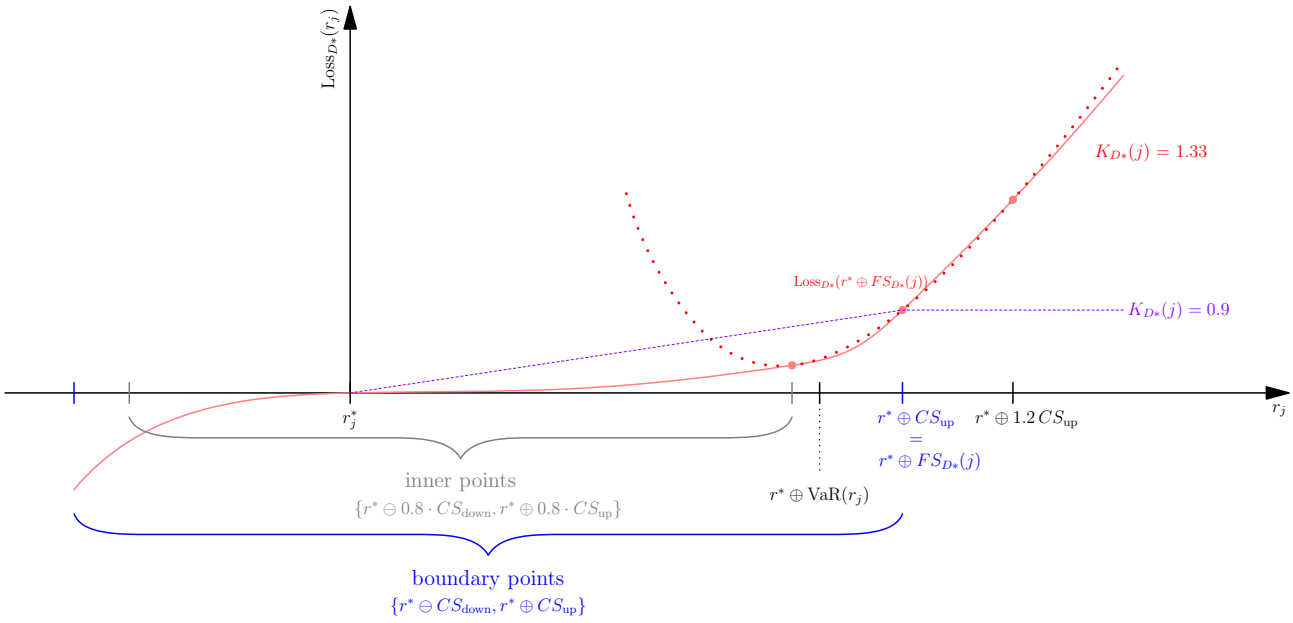

by directly computing the expected shortfall of the losses, i.e. via the direct method. For risk factors with more than 200 returns in the stress period, results showed that our methodology ensures a level of capitalisation comparable to the one resulting from the direct method. For example, one bank participating in the data collection exercise which made its results public [Int20], obtained a total stress scenario risk measure by applying the historical method (with a grid for Θ also having 20%, 40% and 60% of the boundaries) which was only 1% higher than when calculating the expected shortfall of the losses with the direct method, for both linear and structured interest rate strategies.

2.2.5 Obtaining $SS_{10\text{d}}$ when $FS_{D*}(j)$ is at the inner points of Θ

Where the extreme scenario of future shock corresponds to one of the inner points, we are left with no clear guess how $l_j(x)$ might possibly look, apart from the indication that the worst losses presumably do not occur for the most extreme returns of the NMRF. Possible refinements of our strategy could require the evaluation of $l_j(x)$ at further grid points at this stage to get a clearer picture, but to keep the methodology light and simple in line with the goals, our approach refrains from such extensions. This choice has been made also considering that, as mentioned, losses are in general directional in the risk factors - hence, $FS_{D*}(j)$ is rarely expected to be in the inner points of Θ. Instead, we make the blunt assumption that the scenario of future shock at the inner points of Θ is representative for the worst 2.5% losses and set the 10-day SSRM to the corresponding loss,

$$SS_{10\text{d}}(j) = l_j(FS_{D*}(j)) \quad \text{if} \quad FS_{D*}(j) \in \{-0.8\,CS_{\text{down}}(j), 0.8\,CS_{\text{up}}(j)\}\ , \tag{28}$$

accepting that this could underestimate, or overestimate, $\text{ES}(l_j(X))$ slightly.

3 Corner cases and maximum loss approach

As mentioned before, the methodology is expected to work reasonably well in the vast majority of cases. However, special cases could also occur. For example, a very rare case would occur when all four points from the grid Θ lead to zero or negative losses, i.e. actual gains. In this rare situation, we set the 10-day SSRM for the risk factor j to zero:

$$SS_{10\mathrm{d}}(j) = 0 \quad \text{if} \quad l_j(FS_{D*}(j)) \leq 0\,. \tag{29}$$

In addition, when putting forward our methodology, we introduced some assumptions. Assumption A1 and A2, i.e. the identification of the SSRM portfolio and of the NMRFs via the RFET, are prerequisites envisaged in the FRTB. Unlike A1 and A2, A3 and A4 are assumptions that may not be met in practice; for example, there could be shocks for which the pricers of a bank are not able to calculate the corresponding loss, and there could be NMRFs with less than 12 observations in the stress period. [EBA20b] covers those cases by means of additional provisions making our methodology even more complete. To address cases where the pricers cannot determine the loss corresponding to a shock, [EBA20b] set out that banks are to use sensitivity based pricing methods. However, a sensitivity based loss can be computed only in relation to those instruments for which the pricers do not work - this to reflect cases where for the same shock, the pricers of some instruments provide the loss results, while for others they do not, as that shock would lead to arbitrage conditions in the context of those instruments (e.g. because only the NMRF is shocked, and all other risk factors are held constant). For NMRFs with less than 12 returns in the stress period, [EBA20b] envisages a fallback approach which relies on our methodology. Depending on the nature of the risk factor, CS_{up} and CS_{down} under such a fallback approach are either based on the FRTB standardised approach pre-defined shocks or on the shocks calibrated on the returns of a 'similar risk factor' for which at least 12 returns are available. Once those shocks are identified, our methodology is applied in the same way as for risk factors for which more than 12 returns in the stress period are available. Considering that the assumption A4 addresses a problem that may also occur in the ES for modellable risk factors, and that the fallback approach leads back to our methodology, we decided this paper need not be focused on those ad-hoc solutions.

More generally, to address rare cases where supervisors are not satisfied, paragraph 33.16(3) of the FRTB foresees the possibility for supervisors to require a bank to set the stress scenario risk measure to the maximum loss that can occur due to a NMRF. This may happen e.g. when the worst loss for a change in an NMRF occurs as a result of a small change to its current value, far below the 80% of the calibrated shock, or when the SSRM portfolio composition is such that the loss profile for a NMRF cannot be duly captured by the methodology as it could be for very exotic options. Whenever there is a need to, the supervisor could revert to the maximum loss. However, the maximum possible loss could be infinite and a sensible finite replacement is needed. To this end [EBA20b] stipulates that where the maximum loss is infinite, banks are to identify a VaR(99.95) of the losses that may occur due to the NMRF on the 10-business-day horizon rescaled to the NMRF's liquidity horizon. In Table 2 in Section 5, we show how the ES(97.5%) compares to the VaR(99.95%) for a set of SGT distributions.

4 Uncertainty compensation factor

In order to achieve goals G2 and G7, our methodology incorporates in Eqs. 5, 6, 9, and 10, an 'uncertainty compensation factor' $UCF(N_{\mathrm{eff}})$ which is greater than 1 and increases when the number of effective returns N_{eff} decreases – where $N_{\mathrm{eff}} = N$ in the historical method, while $N_{\mathrm{eff}} = N_{\mathrm{up/down}}$ under the asymmetrical sigma method. We keep denoting with N the number of returns in X^j.

In this section, we derive a general approximative formula for the uncertainty compensation factor to compensate the sampling error in obtaining the shocks $CS_{\mathrm{down}}(j)$ and $CS_{\mathrm{up}}(j)$, while it also implicitly covers the generally lower market observability of non-modellable risk factors and approximations in the methodology (such as those introduced to derive the non-linearity coefficient $K_{D*}(j)$).

The sampling error is the difference of an estimator for a sample metric $\widehat{M}$ and the true but unknown value M^*. For our methodology, $\widehat{M}$ is an estimator for the ES given the 10-business day returns, i.e. $\widehat{ES}_{\text{down,up}}$ or $\widehat{AS}_{\text{down,up}}$, and M^* is the true (but unknown) ES for the (unknown) 10-day return parent distribution X.

$\widehat{M}(N, X)$ is called a consistent estimator, if the infinite sample size value converges in probability to the true value, $\lim_{N\to\infty} \widehat{M}(N, X) \overset{\text{prob}}{=} M^*$. The historical ES estimators are consistent. On the contrary, the asigma estimator is in general not consistent[5].

$\widehat{M}(N, X)$ is a (mean) unbiased estimator of M^*, if its expectation (for a certain N) is the true value, i.e. $\mathbb{E}\left(\widehat{M}(N, X)\right) = M^*$. Both the historical and asigma estimators are somewhat biased for finite N, in particular, the historical ES estimators are biased towards zero.

We start with the general uncertainty compensation factor $U_{\alpha^{\text{UC}}}\left(\widehat{M}(N, X)\right)$, which ensures that when multiplying the sampling metric $\widehat{M}(N, X)$ calculated from N independent and identically distributed (i.i.d.) samples of a parent distribution X with it, a certain target confidence level $CL^{\text{UC}} = 1 - \alpha^{\text{UC}}$ for not underestimating the true value $M^*(X)$ is achieved. For the asigma method, $N = N_{\text{down,up}}$ can be as low as six and $U_{\alpha^{\text{UC}}}$ becomes substantial. For ease of notation, the dependence on N of $\widehat{M}$ is not always written out.

We set:

$$U_{\alpha^{\text{UC}}}\left(\widehat{M}\right) := \frac{M^*}{q_{\alpha^{\text{UC}}}\left(\widehat{M}\right)}, \tag{30}$$

which ensures

$$P\left(U_{\alpha^{\text{UC}}}\,\widehat{M} \le M^*\right) = P\left(\widehat{M} \le q_{\alpha^{\text{UC}}}\left(\widehat{M}\right)\right) = \alpha^{\text{UC}}, \tag{31}$$

the last equation being the definition of the quantile for a continuous probability distribution.

$U_{\alpha^{\text{UC}}}\left(\widehat{M}(N, X)\right)$ depends on the tail probability α^{UC} and via the quantile $q_{\alpha^{\text{UC}}}\left(\widehat{M}\right)$ on the estimator $\widehat{M}(N, X)$ and thus, on the number of samples N for the estimation and the properties of X.

The quantile $q_{\alpha^{\text{UC}}}$ can be approximated with the Cornish-Fisher expansion [CF38, FC60] in the moments of $\widehat{M}$:

$$q_{\alpha^{\text{UC}}}\left(\widehat{M}\right) = E\left(\widehat{M}\right) + \sigma\left(\widehat{M}\right)\left[z_{\alpha^{\text{UC}}} + H\left(z_{\alpha^{\text{UC}}}, \widehat{M}\right)\right], \tag{32}$$

where σ is the standard deviation and $z_{\alpha^{\text{UC}}} = \Phi^{-1}(\alpha^{\text{UC}})$ denotes the standard normal quantile for tail probability α^{UC}. The terms capturing adjustments to the normal quantile are summarised in

$$\begin{aligned} H\left(z_{\alpha^{\text{UC}}}, \widehat{M}\right) := \frac{1}{6}\left(\left(z_{\alpha^{\text{UC}}}\right)^2 - 1\right) s\left(\widehat{M}\right) + \frac{1}{24}\left(\left(z_{\alpha^{\text{UC}}}\right)^3 - 3z_{\alpha^{\text{UC}}}\right) k\left(\widehat{M}\right) \\ + \frac{1}{36}\left(2\left(z_{\alpha^{\text{UC}}}\right)^3 - 5z_{\alpha^{\text{UC}}}\right) s\left(\widehat{M}\right)^2 + \tilde{H}_{n>4}\left(z_{\alpha^{\text{UC}}}, K_{n>4}\right), \end{aligned} \tag{33}$$

where $s\left(\widehat{M}\right)$ denotes the normalised skewness and $k\left(\widehat{M}\right)$ the excess normalised kurtosis of the distribution of $\widehat{M}$. Eq. 33 is a commonly used expression of the Cornish-Fisher expansion with the terms of the first four cumulants written out explicitly (adjustments I and II on p. 214 of [FC60]), while the contributions from cumulants of fifth and higher order are denoted by $\tilde{H}_{n>4}\left(z_{\alpha^{\text{UC}}}, K_{n>4}\right)$.

If $\widehat{M}$ was normally distributed there were no adjustments to the normal quantile, $H\left(z_{\alpha^{\text{UC}}}, \widehat{M}\right) = 0$, and $s\left(\widehat{M}\right) = 0$ and all higher moments were zero.

For the sampling distribution of the historical ES estimator $\widehat{ES}_{\text{down,up}}(X^j, \alpha)$ one can find results for the asymptotic large N behaviour in the literature. For continuous distributions and finite variance, the historical ES estimator approaches the normal distribution in the large sample limit [MH05, BJPZ08] and asymptotic approximations for the sample variance and confidence intervals are known [MH05, BJPZ08]. Note that because the order statistics $X_{(i)}$ in the tail are highly dependent, this convergence does not follow immediately from the central limit theorem. In [BS08] empirical confidence regions for VaR and ES were investigated for $N \ge 500$.

We are not aware of comparable results for the asigma estimator $\widehat{AS}_{\text{down,up}}$, while our simulations show convergence to the normal distribution (cf. Figure 3). Its first term $\widehat{\mu}_{X^j_{\text{down,up}}}$ is the ES at the 50% tail

[5]For example, in light of the results provided in Section 5, where the return distribution X is set to an SGT distribution and the constant $C_{\text{ES}}^{\text{asigma}}$ in the asigma method is not matching the value such that for that distribution $\widehat{AS}(X, N) \overset{\text{prob}}{\to} \text{ES}(X)$.

Figure 3: Sampling distributions for the asigma method, i.e. using the estimator $\widehat{M} = \widehat{AS}_{\text{down}}$ for different number N of returns X drawn from an SGT distribution, sampled $2 \cdot 10^5$ times. The convergence to the normal distribution is apparent for the largest N. The long dashed black vertical line is the true value M^*, the short dashed grey vertical line is the large N limit $\widehat{M}(N = \infty)$ (exhibiting a bias due to the choice of $C_{\text{ES}}^{\text{asigma}} = 3$), and the vertical dotted lines indicate the median values $\text{med}\left(\widehat{M}\right)$ of the sampling distributions for the different N.

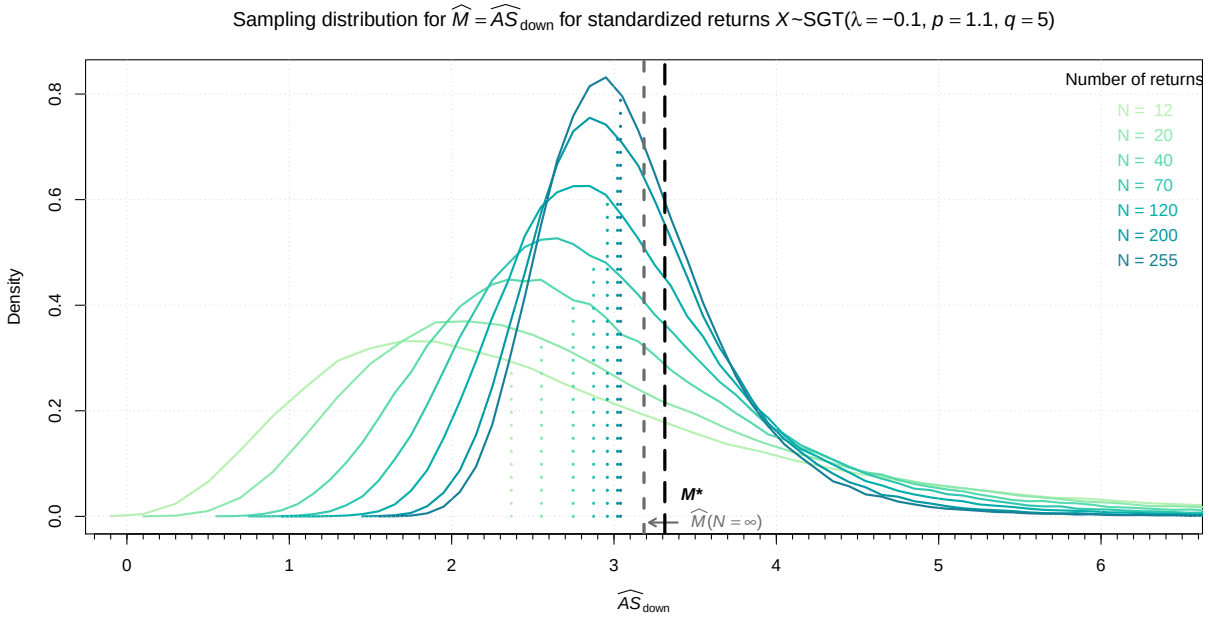

probability. For the second term $\widehat{\sigma}_{X^j_{\text{down}}}$ we can argue that the returns below resp. above the median are identical and only weakly dependent when N gets larger. For i.i.d. normal returns $\widehat{\sigma}_{X^j_{\text{down}}}$ would follow a χ distribution which in turn converges to a normal distribution. For non-normal i.i.d. distributions, the sampling distribution of the variance cannot be described simply [Dou09]. Proposition 5.7 of [Dou09] gives a general formula for the skewness of the sample variance which implies it is always positive. As we will see, the most relevant effects for our purposes involve the skewness $s\left(\widehat{M}\right)$ of the sample distribution, which we also find to be always positive.

For a finite number of returns with $12 \leq N \leq 255$ the large N limit is not reached in any case. Thus, $\widehat{M}(N, X)$ is not normally distributed and $H\left(z_{\alpha^{\text{UC}}}, \widehat{M}\right)$ is not zero even for parent distributions X close to the normal distribution. $H\left(z_{\alpha^{\text{UC}}}, \widehat{M}\right)$ gets smaller for larger N, concomitantly with $\sigma\left(\widehat{M}\right)$, $s\left(\widehat{M}\right)$, and $k\left(\widehat{M}\right)$ all getting smaller, cf. Figure 3.

Figure 3 illustrates the sample distributions $\widehat{M}(N, X)$ for some N in the asigma method, i.e. $\widehat{M} = \widehat{AS}_{\text{down}}$, when the returns X follow a typical skewed and moderately fat-tailed SGT distribution (cf. Section 5). One can see the convergence to the GAUSSian distribution. $U_{50\%}\left(\widehat{M}\right) = \frac{M^*}{\text{med}\left(\widehat{M}\right)}$ can be read off as the true value M^* (dashed) divided by the median values $\text{med}\left(\widehat{M}\right)$ (dotted), as the median is the 50% quantile. Qualitatively, for all $\widehat{M}(N, X)$, i.e. the asigma (Figure 3) and the historical method (not shown) and for both downward and upward shocks, the sample distributions look similar. One can see that the sampling uncertainty increases strongly as N decreases. Yet, even for $N = 12$, the asigma method still delivers acceptable results (using only six values below or above the median!).

We checked with numerical simulations using SGT distributions (cf. Section 5) for X and values $12 \leq N \leq 255$ that the forth order CORNISH-FISHER approximation for the quantile $q_{\alpha^{\text{UC}}}\left(\widehat{M}\right)$ works generally well for $\widehat{M} = \widehat{ES}_{\text{down,up}}$ and $\widehat{M} = \widehat{AS}_{\text{down,up}}$. Deviations from large N simulated quantile values above 10% occurred only for $N \lesssim 40$ (i.e. where the convergence in N to the normal distribution is still far) together with high skewness and kurtosis of X, which leads to high skewness and kurtosis in $\widehat{M}$, as seen in Figure 3, which in turn

causes a deterioration of the CORNISH-FISHER approximation, cf. [Mai18]).

Inserting Eq. 32 in Eq. 30 leads to

$$U_{\alpha^{\mathrm{UC}}}(\widehat{M}) = \frac{M^*}{E\left(\widehat{M}\right) + \sigma\left(\widehat{M}\right)\left[z_{\alpha^{\mathrm{UC}}} + H\left(z_{\alpha^{\mathrm{UC}}}, \widehat{M}\right)\right]}\,. \tag{34}$$

Reducing by M^* and rearranging gives $U_{\alpha^{\mathrm{UC}}}(\widehat{M}) = \left(1 + \frac{E\left(\widehat{M}\right)-M^*}{M^*} + \frac{\sigma\left(\widehat{M}\right)}{M^*}\left[z_{\alpha^{\mathrm{UC}}} + H\left(z_{\alpha^{\mathrm{UC}}}, \widehat{M}\right)\right]\right)^{-1}$.

For moving from this general expression towards an approximative simpler expression we investigate the individual terms.

The term $\frac{E\left(\widehat{M}\right)-M^*}{M^*}$ corrects a bias in the estimator, and is small for the historical method as well as in the asigma method with a suitable constant $C_{\mathrm{ES}}^{\mathrm{asigma}}$. However, the estimator of the asigma method is somewhat conservative for near GAUSSian returns X as discussed in Section 5, so that we need to keep the bias term, which is also dependent on N (cf. Figure 3).

Due to the convergence to the normal distribution and the central limit theorem the term $\sigma\left(\widehat{M}\right)$ will lead to an N_{eff} dependency $\sigma\left(\widehat{M}\right) \propto \frac{1}{\sqrt{N_{\mathrm{eff}}-1.5}}$ – where we are using the approximately unbiased sample estimator [GT71] for the standard deviation with $N_{\mathrm{eff}} - 1.5$ instead of $N_{\mathrm{eff}} - 1$ in the denominator.

In our methodology we target confidence levels $CL^{\mathrm{UC}} = 1 - \alpha^{\mathrm{UC}} \approx 50\%$ that $\widehat{M}$ does not underestimate the true value, in order to achieve the accuracy goal G6. The normal quantile is small in this case, $z_{\alpha^{\mathrm{UC}}\approx 50\%} \approx 0$. The adjustment to the normal quantile $H\left(z_{\alpha^{\mathrm{UC}}}, \widehat{M}\right)$ decreases in N when converging to the normal distribution. However, $\widehat{M}$ is not truly normal for finite N, thus $H\left(z_{\alpha^{\mathrm{UC}}}, \widehat{M}\right)$ is not vanishing completely.

Smallness of the terms described allows using the first order approximation $\frac{1}{1+\varepsilon} \approx 1 - \varepsilon$ for $\varepsilon \ll 1$, and we arrive at the following approximation for the uncertainty compensation:

$$U_{\alpha^{\mathrm{UC}}}(\widehat{M}) \approx 1 + \frac{M^* - E\left(\widehat{M}\right)}{M^*} - \frac{\sigma\left(\widehat{M}\right)}{M^*}\left[z_{\alpha^{\mathrm{UC}}} + H\left(z_{\alpha^{\mathrm{UC}}}, \widehat{M}\right)\right]\,. \tag{35}$$

For confidence levels around 50%, skewness remains as the main driver of $H\left(z_{\alpha^{\mathrm{UC}}\approx 50\%}, \widehat{M}\right)$ when ignoring higher corrections: $H\left(z_{\alpha^{\mathrm{UC}}\approx 50\%}, \widehat{M}\right) \approx \frac{-s\left(\widehat{M}\right)}{6} < 0$, as all sampling distributions $\widehat{M}$ have positive skewness (cf. Figure 3). We get

$$U_{\alpha^{\mathrm{UC}}\approx 50\%}\left(\widehat{M}\right) \approx 1 + \frac{M^* - E\left(\widehat{M}\right)}{M^*} + \frac{\sigma\left(\widehat{M}\right)}{M^*}\frac{s\left(\widehat{M}\right)}{6}\,. \tag{36}$$

We found from numerical simulations of a wide range of standardised SGT distributions (cf. Section 5) that in the range $12 \le N \le 255$ the sampling standard deviation $\hat{\sigma}\left(\widehat{M}\right) \propto (N_{\mathrm{eff}} - 1.5)^{-\xi_\sigma}$ with $(0.45 \le \xi_\sigma^{\mathrm{ES}} \le 0.5)$ for the historical method and $(0.35 \le \xi_\sigma^{\mathrm{asigma}} \le 0.5)$ for the asigma method, as shown in Figure 4. The stronger the non-normality of the returns X, the larger the deviation from the asymptotic normal distribution exponent $\frac{1}{2}$.

For the sampling skewness we find similarly $\hat{s}\left(\widehat{M}\right) \propto (N_{\mathrm{eff}} - 1.5)^{-\xi_{\mathrm{s}}}$ with the exponent ξ_{s} with $(0.45 \le \xi_{\mathrm{s}}^{\mathrm{ES}} \le 0.5)$ for the ES and $(0.1 \le \xi_{\mathrm{s}}^{\mathrm{asigma}} \le 0.5)$ for the asigma method, as shown in Figure 5. There are different sampling skewness (and kurtosis) estimators as discussed in [JG98], which yield almost the same numbers for the high number of samples analysed here $(2 \cdot 10^5)$. The stronger the non- normality of the returns X, the larger the deviation from the asymptotic normal distribution exponent $\frac{1}{2}$ as well.

As shown above, for confidence levels $CL^{\mathrm{UC}} \approx 50\%$, the N_{eff}-dependence of $U_{\alpha^{\mathrm{UC}}}$ is driven by the product $\sigma\left(\widehat{M}\right) s\left(\widehat{M}\right) \propto (N_{\mathrm{eff}} - 1.5)^{-(\xi_\sigma + \xi_{\mathrm{s}})}$ with $0.45 \lesssim \xi_\sigma + \xi_{\mathrm{s}} \le 1$. For other confidence levels, $z_{\alpha^{\mathrm{UC}}}$ gets larger and the N_{eff} dependence of $U_{\alpha^{\mathrm{UC}}}$ is therefore not mostly dependent on the skewness, but also on the standard deviation and higher moments, cf. Eq. 33.

To simplify our methodology in line with goal G2 we universally use the N_{eff} dependence $(N_{\mathrm{eff}} - 1.5)^{-\frac{1}{2}}$ for both the historical and asigma method and attaining goal G7. This choice is better in line with the exponent found for the asigma method, in which the uncertainty compensation factor is more relevant, as N_{eff} is smaller.

Figure 4: Sampling standard deviation of the sampling distribution for the estimator $\widehat{M} = \widehat{ES}_{\text{down}}$ used in the historical method (top) and $\widehat{M} = \widehat{AS}_{\text{down}}$ in the asigma method (bottom) versus number of returns N. $2 \cdot 10^5$ samples of size N were drawn for each N from various SGT distributions (coloured dots) including a Gaussian (grey dots) - on both axes logarithmic scales are used. The squares indicate fixed exponents $\xi_\sigma^{\text{ES}} = \{0.45, 0.5\}$ (top) and $\xi_\sigma^{\text{asigma}} = \{0.35, 0.5\}$ (bottom). In both cases, the sampled $\hat{\sigma}\left(\widehat{M}\right) \propto (N_{\text{eff}} - 1.5)^{-\xi_\sigma}$ describe the variation of the sampling standard deviation well. For a Gaussian distribution, the exponent for both estimators is very close to $\frac{1}{2}$.

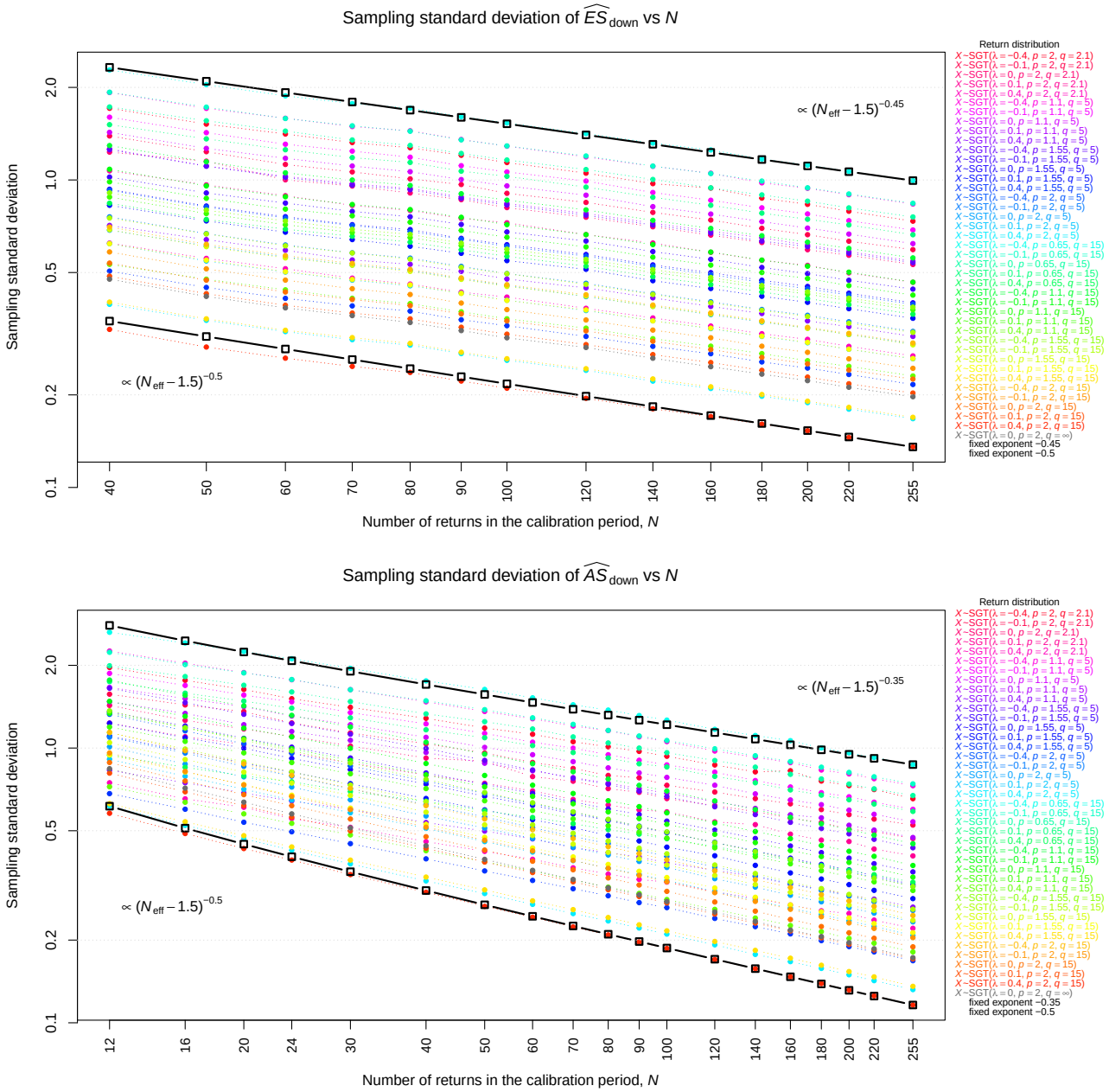

Figure 5: Sampling skewness of the sampling distribution, $\hat{s}\left(\widehat{M}\right)$, for the estimator $\widehat{M} = \widehat{ES}_{\text{down}}$ used in the historical method (top) and $\widehat{M} = \widehat{AS}_{\text{down}}$ in the asigma method (bottom) versus number of returns N - on both axes logarithmic scales are used. $2 \cdot 10^5$ samples of size N were drawn for each N from various SGT distributions (coloured dots) including a Gaussian (grey dots). The squares indicate fixed exponents $\xi_{\text{s}}^{\text{ES}} = \{0.45, 0.5\}$ (top) and $\xi_{\text{s}}^{\text{asigma}} = \{0.1, 0.5\}$ (bottom). In both cases, the sampled $\hat{s}\left(\widehat{M}\right) \propto (N_{\text{eff}} - 1.5)^{-\xi_{\text{s}}}$ describe the variation of the skewness overall well. For very non-Gaussian and skewed SGT distributions, sampling noise and deviations are visible. For a Gaussian distribution, the exponent for both estimators is close to $\frac{1}{2}$.

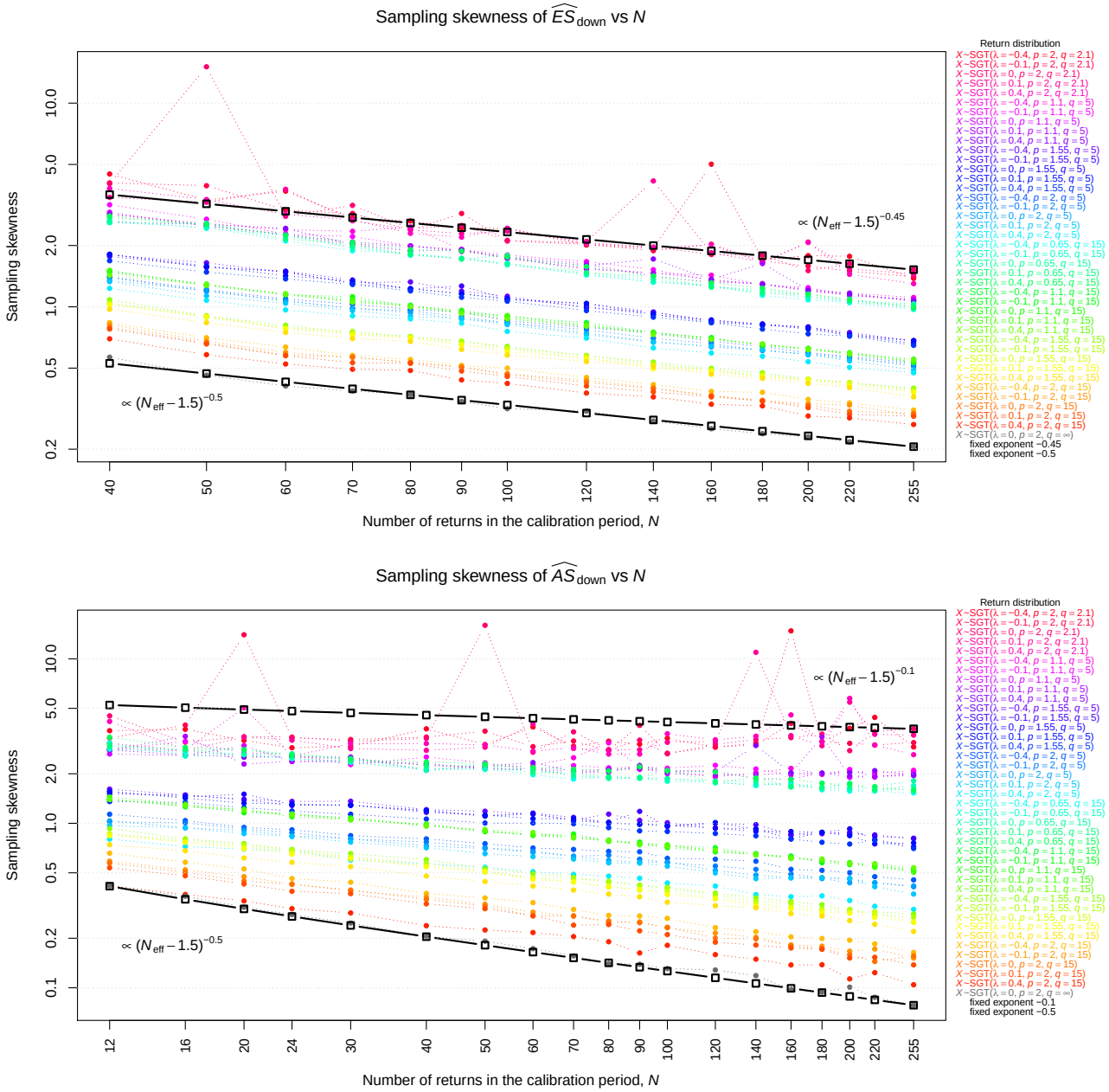

For the historical method, the exponent could be chosen higher. Overall, it is a prudent choice covering both methods and non-normal returns well.

Based on these considerations, we make the following ansatz for the general approximative expression for the uncertainty compensation factor in our methodology:

$$U_{\alpha^{\mathrm{UC}}}\left(\widehat{M}\right) \approx C_{\mathrm{A}}^{\mathrm{UC}}\left(CL^{\mathrm{UC}}, \widehat{M}\right) + \frac{C_{\mathrm{B}}^{\mathrm{UC}}\left(CL^{\mathrm{UC}}, \widehat{M}\right)}{\sqrt{N_{\mathrm{eff}} - 1.5}}\,. \tag{37}$$

with positive calibration constants $C_{\mathrm{A}}^{\mathrm{UC}}\left(CL^{\mathrm{UC}}, \widehat{M}\right)$ and $C_{\mathrm{B}}^{\mathrm{UC}}\left(CL^{\mathrm{UC}}, \widehat{M}\right)$.

To define the uncertainty compensation factor $UCF(N_{\mathrm{eff}})$ that is finally used in Eqs. 5, 6, 11, and 12, we decided to further simplify Eq. 37 by setting single calibration constants for $CL^{\mathrm{UC}} \approx 50\%$ and all $\widehat{M}(N, X)$ in accordance with Goals G1 and G2:

$$UCF(N_{\mathrm{eff}}) = C_{\mathrm{A}}^{\mathrm{UC}} + \frac{C_{\mathrm{B}}^{\mathrm{UC}}}{\sqrt{N_{\mathrm{eff}} - 1.5}}\,, \tag{38}$$

with $C_{\mathrm{A}}^{\mathrm{UC}} = 0.95$ and $C_{\mathrm{B}}^{\mathrm{UC}} = 1$. In Section 5 we motivate the choice of the two constants and check that the confidence level $CL^{\mathrm{UC}} \approx 50\%$ is indeed obtained.

5 Motivating the methodology constants using SGT distributions

The methodology and the uncertainty compensation factor depend on some parameters. Those parameters should be set so as to meet our goals. In this section, we discuss and motivate the values at which they were set by investigating SGT distributions. In Annex A, the definition of the density of the SGT distributions is provided in a parametrisation which is suitable for the R language [R C19]. It also provides explicit expressions for the first four moments, VaR, and ES.

It is a well known stylised fact that return distributions of financial risk factors are often strongly non-normal. A generalisation of the Student-t distribution are the skewed generalised t (SGT) distributions, which describe strongly skewed and heavy tailed financial returns well [The98, HMN10, KM13, AMLSG16, MM17]. While the SGT family is perhaps the most used, there are several other generalisations of the Student-t distribution [LN20].

Studies of SGT distributions for financial risk factors typically use stock market data (e.g. [The98, HMN10, AMLSG16, MM17]), probably because of their good availability. However, goal G1 states that the methodology should be universal. [EBA19, EBA20a] analysed a wide variety of risk factors (almost 50,000 in total) across all risk classes (foreign exchange, interest rates, equity and commodities) used in the regulatory capital market risk models in some of the largest European banks. The analysis in [EBA20a] showed that risk factor returns on the 10-business-day horizon are often strongly skewed and leptokurtic and that the SGT distributions can be used to describe the 10-day returns well.

Accordingly, aiming at setting the methodology's parameters, we first provide explicit expressions for the VaR and ES of SGT distributions. Making use of those analytical results, and leveraging on the historical risk factor data analysed in [EBA20a], we motivate the choices made on the values set for $C_{\mathrm{ES}}^{\mathrm{asigma}}$ in Eqs. 11 and 12, ϕ^{asigma} in Eq. 25, $C_{\mathrm{A}}^{\mathrm{UC}}$ and $C_{\mathrm{B}}^{\mathrm{UC}}$ in Eq. 38. We also back our choice on the step width h employed to derive the coefficient Γ in Eq. 22, and assess the confidence level prescribed in [EBA20b] for calculating a maximum possible loss when such loss is infinite as described in subsection 3.

5.1 VaR and ES of SGT distributions

SGT distributions form a location-scale family that encompasses many other distributions e.g. the normal distribution and Student's t distribution. In this paper (see Annex A for more details), we use the notation in the following independent parameters: μ, σ, λ, p, and q. μ and σ are the mean and standard deviation, λ with $-1 < \lambda < 1$ is the skewness parameter, $p > 0$ is the peakedness, and $q > 0$ the tail thickness parameter. In Annex A, we show (Eqs. 64 and 65) that the ES and VaR for SGT distributions can be expressed as:

$$\mathrm{ES}^{\mathrm{SGT}}(\alpha;\mu,\sigma,\lambda,p,q) = -\mu + C_{\mathrm{ES}}^{\mathrm{SGT}}(\alpha;\lambda,p,q)\sigma\,, \tag{39}$$

and

$$\mathrm{VaR}^{\mathrm{SGT}}(\alpha;\mu,\sigma,\lambda,p,q) = -\mu + C_{\mathrm{VaR}}^{\mathrm{SGT}}(\alpha;\lambda,p,q)\sigma\,. \tag{40}$$

with explicit constants $C_{\mathrm{ES}}^{\mathrm{SGT}}$ and $C_{\mathrm{VaR}}^{\mathrm{SGT}}$ in Eqs. 39 and 40 capturing the terms depending on the shape of the normalised distribution and the tail probability α.

The SGT distributions split at the median have the same location and volatility scale properties and thus, the same ansatz of the ES being a linear function of mean and standard deviation on the support below or above the median *med* is used for the asigma method, while we do not have analytical expressions. We thus write for the asigma method:

$$\mathrm{ES}^{\mathrm{SGT}}(\alpha;\mu,\sigma,\lambda,p,q) = -\mu^{\mathrm{asigma}}_{\mathrm{down/up}:X>/\leq med} + C_{\mathrm{ES}}^{\mathrm{SGT,asigma}}(\alpha;\lambda,p,q)\sigma^{\mathrm{asigma}}_{\mathrm{down/up}:X>/\leq med}\,, \tag{41}$$

We recall that the analogue of the mean $\mu^{\mathrm{asigma}}_{\mathrm{down/up}:X>/\leq med}$ and the analogue of the standard deviation $\sigma^{\mathrm{asigma}}_{\mathrm{down/up}:X>/\leq med}$ are computed on the arguments below or above the median in the asigma method.

When making the simplification that the constant $C_{\mathrm{ES}}^{\mathrm{SGT,asigma}}(\alpha;\lambda,p,q)$ can be set to a single constant $C_{\mathrm{ES}}^{\mathrm{asigma}}$, we get the expression for the asigma method estimator in Eqs. 11 and 12. We show detailed numerical results in Subsection 5.2.1.

5.2 Motivating the constants of the methodology

As mentioned, the analysis in [EBA20a] showed that SGT distributions describe well the features observed in risk factor returns on the 10-business-day horizon. Instances of risk factors close to the theoretical Klaassen bound for unimodal distributions [KMv00] in the skewness-kurtosis space were observed. The SGT parameter ranges which overall describe the 10-business-day risk factors returns well [EBA20a] are stated in Table 1, where we also list the parameter sets we analyse concretely. These were compared to the empirical values observed for real financial risk factor data in [EBA20a], to ensure that the SGT distributions we use in our analyses broadly match the third and fourth moments observed in market data. Only parameter combinations leading to finite first four moments, i. e. $pq > 4$ were considered and without loss of generality the standardised distributions, i.e. $\mu = 0$ and $\sigma = 1$, were used.

In other words, we employ the SGT distributions with the set of parameter values shown in Table 1 as a first four moments matched surrogate of all 10-business-day risk factor returns in all risk categories collected in [EBA19, EBA20a] in Pillar 1 market risk models. Together with the explicit expressions for the moments, ES and VaR, we believe that this is an efficient tool-set to assess questions in risk modelling across all risk categories under the FRTB in general.

The set of SGT distributions are used for the following: (i) The asigma method's constants $C_{\mathrm{ES}}^{\mathrm{SGT,asigma}}$ and ϕ^{asigma} motivating the value chosen in the SSRM methodology (additionally, [EBA20a] checked the historical values); (ii) the ratio of VaR(α) over ES(α) which motivates 0.8 used for the inner points in Θ (Eq. 13) and the step width $h = 0.2$ (Eq. 22); (iii) simulation analysis of the probability of underestimating the exact ES or asigma method approximation of it when calculating them from a sample of size N in order to determine the constants in the uncertainty compensation factor formula; (iv) ratio of VaR($1 - 99.95\%$) over ES($\alpha = 2.5\%$). The VaR(99.95%) is used as the finite value replacement in case a maximum loss incurring on shocking a risk factor would be infinite theoretically, cf. Subsection 5.2.4.

Table 2 shows the SGT parameter sets of Table 1 with finite first four moments along with the corresponding normalised skewness, excess kurtosis, VaR(α), ES(α), $C_{\mathrm{ES}}^{\mathrm{SGT,asigma}}$, the tail shape parameter ϕ (cf. Eq. 20), and $\frac{\mathrm{VaR}(1-99.95\%)}{\mathrm{ES}(\alpha)}$ for the standardised distributions for tail probability $\alpha = 2.5\%$. The value $q = \infty$ was numerically approximated by $q = 10^5$. For standardised SGT distributions $\mathrm{ES}(\alpha) = C_{\mathrm{ES}}^{\mathrm{SGT}}(\alpha;\lambda,p,q)$ (cf. Eq. 64). Only the values for the left tail are reported, because the right tail values are the ones for $-\lambda$. Results were obtained using the analytical expressions of Subsection 5.1 or numerically from large samples of size $N = 10^7$.

Table 1: Standardised SGT distribution parameters ranges which overall describe the 10-business-day risk factors returns for all risk factors, and lists of the parameter sets that we analyse in detail if the kurtosis is finite (i.e. $pq > 4$).

Parameter	Lower	Upper	Values analysed
λ (skew)	-0.4	0.4	{ -0.4, -0.1, 0, 0.1, 0.4 }
q (tail thickness)	2.1	∞	{ 2.1, 5, 15, ∞ }
p (peakedness)	0.65	2	{ 0.65, 1.1, 1.55, 2 }

We observe in Table 2 that the ES varies significantly depending on λ and to a lesser extent on p and q, it stays well below the HÜRLIMANN bound [Hür02] which implies $\mathrm{ES}(2.5\%) \leq 6.245$ in our case.

5.2.1 Constants $C_{\mathrm{ES}}^{\mathrm{asigma}}$ and ϕ^{asigma} for the asigma method

While the historical method is parameter free except for the loss evaluation grid and the non-linearity correction specification, the constant $C_{\mathrm{ES}}^{\mathrm{asigma}}$ is the main parameter in the asigma method. The key idea for the asigma method was that even for few returns, a mean and standard deviation can still be estimated below and above the median, when an estimate of the ES becomes infeasible. But then those quantities need to be converted according to Eq. 41 to an approximation of the ES, which varies strongly depending on the distributional properties.

Why this works well in practice using a single constant can be inferred from Figure 6, where the components of the calibrated shock according to the asigma method of Eg. 41 for the set of SGT distribution is plotted along with $\mathrm{ES}(\alpha)$.

Because only the relevant half of the distribution is considered to cater for asymmetry, $\sigma_{\mathrm{down}:X\leq med}^{\mathrm{asigma}}$ picks up a lot of the variation for different SGT parameters, while the variation of $C_{\mathrm{ES}}^{\mathrm{SGT,asigma}}(\alpha;\lambda,p,q)$ in λ for fixed p,q is small. $\mu_{\mathrm{down}:X\leq med}^{\mathrm{asigma}}$ in turn does not depend much on λ and picks up some variation for different p,q, albeit to a lesser degree. The effect of the variations in $\sigma_{\mathrm{down}:X\leq med}^{\mathrm{asigma}}$ and $\mu_{\mathrm{down}:X\leq med}^{\mathrm{asigma}}$ lead to a more stable value $C_{\mathrm{ES}}^{\mathrm{SGT,asigma}}(\alpha;\lambda,p,q)$, which exhibits much less variation than $\mathrm{ES}(\alpha) = C_{\mathrm{ES}}^{\mathrm{SGT}}(\alpha;\lambda,p,q)$. The values for $C_{\mathrm{ES}}^{\mathrm{SGT,asigma}}(\alpha;\lambda,p,q)$ are indeed around 3 for many SGT distributions. Somewhat lower for near normal distributions ($p = 2$, $q = \infty$) and somewhat higher for strongly non-GAUSSIAN cases.

Considering the relatively modest variation of $C_{\mathrm{ES}}^{\mathrm{SGT,asigma}} \approx 3$, for the sake of universality of goal G1 and simplicity of goal G4 of the methodology, a single calibration constant $C_{\mathrm{ES}}^{\mathrm{asigma}} = 3$ was considered overall appropriate for all risk factors. A calibration based on historical risk factor data confirms this choice [EBA20a].

The tail shape parameter ϕ (cf. Eq. 20) can vary very strongly, mainly driven by excess kurtosis. The non-linearity correction, where ϕ enters, can go in both directions, as the loss function could be convex or concave at the outer points of Θ. Therefore, the constant ϕ^{asigma} approximating ϕ in the asigma method for all risk factors should be targeting a typical value as no conservative choice can be made. The value $\phi^{\mathrm{asigma}} = 1.04$ in the asigma method captures typical moderately non-normal distributions well and has the practical advantage that the term $\frac{\phi^{\mathrm{asigma}}-1}{h^2}$ in the non-linearity correction becomes unity for the loss grid step width $h = 0.2$ (cf. Subsection 2.2.4). To conclude the discussion of constants for the asigma method, we note that our analysis based on the SGT distributions is showing a qualitatively similar picture to the historical return data analysis in [EBA20a]. The SGT based analysis captures very well the ranges of the metrics in which we are interested, while the historical data adds information on the frequency of the occurrence of certain distributional features like skewness. For a particular portfolio of financial instruments, only few risk factors might be driving the losses. Therefore, it is important for reaching goal G1 to ensure that the methodology works well for all sets of risk factors, as opposed to on average only.

Table 2: SGT parameters, skewness, excess kurtosis, VaR(α), ES(α), $\frac{\text{VaR}(\alpha)}{\text{ES}(\alpha)}$, ES($\alpha$) $= C_{\text{ES}}^{\text{SGT}}$, $C_{\text{ES}}^{\text{SGT,asigma}}$, tail shape parameter ϕ, and $\frac{\text{VaR}(1-99.95\%)}{\text{ES}(\alpha)}$ for standardised SGT distributions ($\mu = 0$, $\sigma = 1$) with $\alpha = 2.5\%$.

λ	p	q	skew.	ex. kurt.	VaR(α)	ES(α)	$\frac{\text{VaR}(\alpha)}{\text{ES}(\alpha)}$	$C_{\text{ES}}^{\text{SGT,asigma}}$	ϕ	$\frac{\text{VaR}(1-99.95\%)}{\text{ES}(\alpha)}$
-0.4	2	2.1	-2.18	58.27	2.34	3.50	0.67	3.05	1.188	2.24
-0.1	2	2.1	-0.61	32.16	2.09	3.01	0.69	3.00	1.165	2.15
0	2	2.1	0	30.00	1.97	2.80	0.70	2.99	1.146	2.10
0.1	2	2.1	0.61	32.16	1.85	2.57	0.72	2.96	1.134	2.05
0.4	2	2.1	2.18	58.27	1.45	1.87	0.77	2.78	1.084	1.83
-0.4	1.1	5	-2.77	27.25	2.49	3.86	0.65	3.16	1.189	2.28
-0.1	1.1	5	-0.83	17.78	2.19	3.31	0.66	3.15	1.175	2.22
0	1.1	5	0	16.89	2.04	3.05	0.67	3.15	1.165	2.20
0.1	1.1	5	0.83	17.78	1.87	2.76	0.68	3.15	1.159	2.16
0.4	1.1	5	2.77	27.25	1.35	1.86	0.73	3.09	1.112	1.98
-0.4	1.55	5	-1.37	5.16	2.42	3.36	0.72	2.99	1.096	1.90
-0.1	1.55	5	-0.39	3.35	2.16	2.93	0.74	2.96	1.083	1.85
0	1.55	5	0	3.20	2.04	2.74	0.75	2.95	1.078	1.82
0.1	1.55	5	0.39	3.35	1.92	2.54	0.76	2.93	1.072	1.79
0.4	1.55	5	1.37	5.16	1.51	1.89	0.80	2.78	1.047	1.64
-0.4	2	5	-0.88	1.78	2.31	3.02	0.77	2.84	1.060	1.71
-0.1	2	5	-0.24	1.06	2.09	2.67	0.78	2.78	1.050	1.65
0	2	5	0	1.00	1.99	2.52	0.79	2.76	1.047	1.63
0.1	2	5	0.24	1.06	1.89	2.37	0.80	2.72	1.042	1.60
0.4	2	5	0.88	1.78	1.58	1.88	0.84	2.54	1.027	1.47
-0.4	0.65	15	-3.79	40.08	2.54	4.18	0.61	3.25	1.229	2.42
-0.1	0.65	15	-1.21	28.24	2.20	3.58	0.62	3.26	1.225	2.40
0	0.65	15	0	26.96	2.03	3.26	0.62	3.27	1.215	2.39
0.1	0.65	15	1.21	28.24	1.83	2.91	0.63	3.27	1.214	2.37
0.4	0.65	15	3.79	40.08	1.22	1.81	0.67	3.27	1.167	2.22
-0.4	1.1	15	-1.57	5.82	2.52	3.52	0.72	3.04	1.088	1.88
-0.1	1.1	15	-0.46	4.02	2.24	3.07	0.73	3.03	1.081	1.84
0	1.1	15	0	3.85	2.10	2.86	0.73	3.03	1.078	1.82
0.1	1.1	15	0.46	4.02	1.95	2.63	0.74	3.02	1.072	1.79
0.4	1.1	15	1.57	5.82	1.48	1.90	0.78	2.94	1.052	1.67
-0.4	1.55	15	-0.95	1.86	2.38	3.09	0.77	2.84	1.051	1.65
-0.1	1.55	15	-0.27	1.20	2.14	2.73	0.78	2.81	1.045	1.61
0	1.55	15	0	1.14	2.04	2.58	0.79	2.80	1.042	1.59
0.1	1.55	15	0.27	1.20	1.93	2.41	0.80	2.78	1.039	1.57
0.4	1.55	15	0.95	1.86	1.57	1.89	0.83	2.63	1.026	1.47
-0.4	2	15	-0.66	0.59	2.25	2.81	0.80	2.70	1.035	1.53
-0.1	2	15	-0.18	0.26	2.05	2.51	0.82	2.65	1.030	1.49
0	2	15	0	0.23	1.97	2.40	0.82	2.62	1.028	1.47
0.1	2	15	0.18	0.26	1.89	2.27	0.83	2.59	1.025	1.45
0.4	2	15	0.66	0.59	1.61	1.86	0.86	2.42	1.016	1.36
-0.4	0.65	∞	-2.51	14.43	2.64	3.97	0.66	3.20	1.134	2.09
-0.1	0.65	∞	-0.78	10.37	2.30	3.43	0.67	3.22	1.129	2.08
0	0.65	∞	0	9.96	2.13	3.16	0.67	3.23	1.128	2.06
0.1	0.65	∞	0.78	10.37	1.94	2.85	0.68	3.24	1.123	2.04
0.4	0.65	∞	2.51	14.43	1.35	1.87	0.72	3.24	1.097	1.93
-0.4	1.1	∞	-1.27	3.40	2.50	3.34	0.75	2.95	1.061	1.72
-0.1	1.1	∞	-0.37	2.37	2.23	2.94	0.76	2.94	1.056	1.69
0	1.1	∞	0	2.28	2.10	2.75	0.76	2.94	1.054	1.67
0.1	1.1	∞	0.37	2.37	1.96	2.55	0.77	2.93	1.051	1.65
0.4	1.1	∞	1.27	3.40	1.53	1.90	0.81	2.85	1.036	1.55
-0.4	1.55	∞	-0.82	1.13	2.34	2.96	0.79	2.76	1.038	1.55
-0.1	1.55	∞	-0.23	0.69	2.12	2.64	0.80	2.73	1.033	1.52
0	1.55	∞	0	0.65	2.02	2.50	0.81	2.72	1.032	1.50
0.1	1.55	∞	0.23	0.69	1.92	2.35	0.82	2.70	1.029	1.48
0.4	1.55	∞	0.82	1.13	1.59	1.88	0.85	2.56	1.020	1.40
-0.4	2	∞	-0.58	0.25	2.22	2.71	0.82	2.63	1.027	1.46
-0.1	2	∞	-0.16	0.02	2.04	2.45	0.83	2.58	1.023	1.42
0	2	∞	0	0.00	1.96	2.34	0.84	2.55	1.021	1.41
0.1	2	∞	0.16	0.02	1.88	2.22	0.85	2.52	1.019	1.39
0.4	2	∞	0.58	0.25	1.62	1.85	0.87	2.36	1.013	1.31

Figure 6: Asigma method components $\mu^{\text{asigma}}_{\text{down:}X\leq med}$ $\sigma^{\text{asigma}}_{\text{down:}X\leq med}$ $C^{\text{SGT,asigma}}_{\text{ES}}$ to obtain the expected shortfall for SGT distributions. $\sigma^{\text{asigma}}_{\text{down:}X\leq med}$ explains a large part of the variation of the ES. Thus, $C^{\text{SGT,asigma}}_{\text{ES}}$ (black squares) shows much less variation than the ES. Finally, $C^{\text{SGT,asigma}}_{\text{ES}} \approx 3$ for many SGT distributions, while being conservative for near normal distributions ($p = 2$, $q = \infty$).

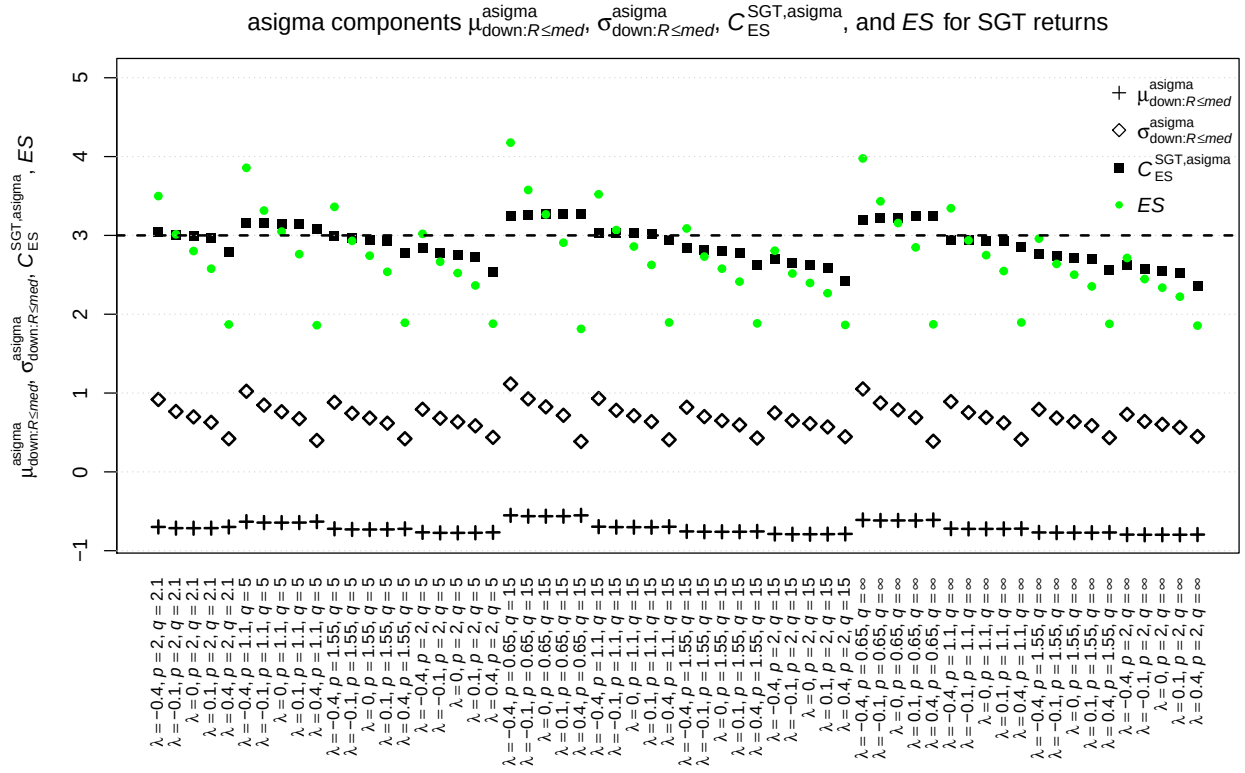

5.2.2 Constants for the uncertainty compensation factor

To fulfil goals G1 and G4 for a universally applicable yet simple methodology, we want to further simplify Eq. 35 by choosing universal constants $C_{\mathrm{A}}^{\mathrm{UC}}$ and $C_{\mathrm{B}}^{\mathrm{UC}}$ for all risk factors:

$$U_{\alpha^{\mathrm{UC}}}\left(\widehat{M}(N,X)\right) \approx C_{\mathrm{A}}^{\mathrm{UC}}\left(\widehat{M},X\right) + \frac{C_{\mathrm{B}}^{\mathrm{UC}}\left(CL^{\mathrm{UC}},\widehat{M}(N,X)\right)}{\sqrt{N_{\mathrm{eff}}-1.5}} = C_{\mathrm{A}}^{\mathrm{UC}} + \frac{C_{\mathrm{B}}^{\mathrm{UC}}}{\sqrt{N_{\mathrm{eff}}-1.5}}\,. \tag{42}$$

where we recall that $N_{\mathrm{eff}} = N$ for $N \geq N^{\mathrm{hist}} = 200$, and $N_{\mathrm{eff}} = N_{\mathrm{up/down}}$ for $12 = N^{\mathrm{asigma}} \leq N \leq N^{\mathrm{hist}}$.

We start with the large N limit and $C_{\mathrm{A}}^{\mathrm{UC}}$. The TARGET2 real-time gross settlement system owned and operated by the Eurosystem has typically at least 255 operating days per calendar year, so that $M = 256$ observations and $N = 255$ returns is a reasonable choice for the largest number of returns in a year. In line with the calibration goal G3, the uncertainty compensation for daily data should be close to one, while a bit higher to cater for non-sampling related uncertainty stemming from the lower observability of NMRF,

$$U_{\alpha^{\mathrm{UC}}}\left(\widehat{M}(N=255)\right) \approx 1\,. \tag{43}$$

Consequently, the constant $C_{\mathrm{A}}^{\mathrm{UC}}$ needs to be smaller than one and is connected with $C_{\mathrm{B}}^{\mathrm{UC}}$.

We set the constants $C_{\mathrm{A}}^{\mathrm{UC}} = 0.95$ and $C_{\mathrm{B}}^{\mathrm{UC}} = 1$ in Eq. 42 for both estimators $\widehat{M} = \widehat{ES}_{\mathrm{left,right}}$ and $\widehat{M} = \widehat{AS}_{\mathrm{down,up}}$ used for determining the calibrated shocks. For ensuring that $U_{\alpha^{\mathrm{UC}}}$ actually provides the desired level of uncertainty compensation, we use the ansatz in Eq. 42 and simulate the probability of underestimation

$$P\left(\widehat{M}U_{\alpha^{\mathrm{UC}}} \leq M^* = \mathrm{ES}_{\alpha^{\mathrm{UC}}}\left(SGT(\lambda,p,q)\right)\right) \tag{44}$$

by drawing from the set of SGT distributions with the parameters of Table 1 which mimic the universe of risk factors. Overall, the target was to ensure the probability of underestimation is generally lower or around 50%, i.e. the median of the sampled calibrated shocks is higher or close to the true value. Annex 1 of [EBA20b] shows details of those simulations performed, which we summarise here.

With $C_{\mathrm{A}}^{\mathrm{UC}} = 0.95$ and $C_{\mathrm{B}}^{\mathrm{UC}} = 1$ for the historical method where $N \geq 200$, $P\left(\widehat{M}U_{\alpha^{\mathrm{UC}}} \leq M^*\right) \lesssim 60\%$ and for the asigma method where $N \geq 12$, $P\left(\widehat{M}U_{\alpha^{\mathrm{UC}}} \leq M^*\right) \lesssim 70\%$. The highest probabilities of underestimation occur for strongly non-Gaussian distributions for which $H\left(z_{\alpha^{\mathrm{UC}}},\widehat{M}\right)$ is more material due to high skewness and/or kurtosis, requiring a higher value for $U_{\alpha^{\mathrm{UC}}}$.

Since the asigma method uses a single constant $C_{\mathrm{ES}}^{\mathrm{asigma}} = 3$, the bias term of Eq. 35 which is implicit in $C_{\mathrm{A}}^{\mathrm{UC}}$ cannot be equally matched for all SGT distributions. Thus, where the correct value for $C_{\mathrm{ES}}^{\mathrm{asigma}}$ is markedly different, the bias term in Eq. 34 leads to stronger deviation of the probability of underestimation from the target level.

At the same time, the values $N_{\mathrm{hist}} = 200$ and $N^{\mathrm{asigma}} = 12$ were considered to be appropriate in combination with the uncertainty compensation factor and the chosen constants $C_{\mathrm{A}}^{\mathrm{UC}}$ and $C_{\mathrm{B}}^{\mathrm{UC}}$. $N^{\mathrm{hist}} = 200$ was also motivated from the notion that in a year having about 255 business days, 55 business days correspond roughly to the Christmas and year-end period plus the northern hemisphere summer holiday period with reduced trading activity.

5.2.3 Step width h

The non-linearity correction described in Subsection 2.2.4 is applied in order to approximate the ES of the tail losses, which implies an integration from the VaR(97.5%) to infinity. Table 2 indicates that $\frac{\mathrm{VaR}(97.5\%)}{\mathrm{ES}(97.5\%)} \approx 0.8$, so that the step width $h = 0.2$ in Eq. 22 approximates VaR(97.5%) overall well.

5.2.4 Confidence level for the maximum loss

For the ratio $\frac{\mathrm{VaR}(1-99.95\%)}{\mathrm{ES}(\alpha)}$ we can infer from Table 2 that it is about 1.4 for the normal distribution, while growing for non-GAUSSian parameter choices up to 2.4. Thus, the approach laid down in Section 3 setting

$SS_{10d}(j)$ to a VaR measure with a 99.95% confidence level targets a level of conservatism that is set to be 1.4 to 2.4 times higher than the one which would result from the application of the historical calibration of the stress scenario risk measure, ignoring the small uncertainty compensation factor.

6 The methodology at bucket level

The regulatory bucketing approach in paragraph MAR 31.16(2) of the FRTB introduces a set of regulatory buckets that a bank can use for proving the modellability of risk factors belonging to curves or surfaces. Where banks apply that approach, they are allowed to determine a single stress scenario for all risk factors in the regulatory bucket. The methodology presented at risk factor level is applicable at bucket level with minimal and natural extensions in line with goal G5.

Assumptions A1, A2 and A3 are still valid. Assumption A4 is slightly revised for the regulatory bucket case by assuming that the bank is able to determine the loss that would suffer due to changes in the values of all the M_B risk factors within the bucket:

$$l(\mathbf{x}) = l(x_1, x_2, ..., x_{M_B}) = \text{Loss}_{D^*}(r_1^* \oplus x_1, r_2^* \oplus x_2, ..., r_{M_B}^* \oplus x_{M_B}) \,, \tag{45}$$

where $\mathbf{x}$ is the vector of shocks $(x_1, x_2, ..., x_{M_B})$ applied to the risk factors $r_1, r_2, .., r_{M_B}$ in the bucket B. The application of those shocks leads to the loss $l(\mathbf{x})$.

The steps of the methodology applicable at single risk factor level are adapted as follows to be applicable at bucket level. Analogously to the single risk factor case, a time series of nearest to 10-business-day returns is determined for each of the M_B risk factors in the bucket B. We denote with N_j, the number of returns in the time series for the risk factor j in the bucket B, and with $N_B = \min(N_1, N_2, ..., N_{M_B})$. Where $N_B \geq N_{\text{hist}} = 200$, a downward calibrated shock $CS_{\text{down}}(j)$ and an upward calibrated shock $CS_{\text{up}}(j)$ are determined with the historical method separately for each of the M_B risk factors in the bucket B. Where $200 = N_{\text{hist}} > N_B \geq N_{\text{asigma}} = 12$, those shocks are determined with the asymmetrical sigma method.

Our methodology finds the extreme scenario of future shocks, among the shifts following the contour of the calibrated shocks of the bucket's risk factors. We define the β downward contoured shift
$\zeta_{\text{down}}(\beta) = (-\beta\, CS_{\text{down}}(1), -\beta\, CS_{\text{down}}(2), ..., -\beta\, CS_{\text{down}}(M_B))$ and the β upward contoured shift $\zeta_{\text{up}}(\beta) = (\beta\, CS_{\text{up}}(1), \beta\, CS_{\text{up}}(2), ..., \beta\, CS_{\text{up}}(M_B))$ and we obtain a set of scenarios Z by spanning β in the interval $[0, 1]$:

$$Z = \bigcup_{\beta \in [0,1]} \zeta_{\text{down}}(\beta) \;\cup \bigcup_{\beta \in [0,1]} \zeta_{\text{up}}(\beta) \,. \tag{46}$$

We decided to focus our search of the extreme scenario of future shocks among the contoured shifts to reflect that in reality, shifts for risk factors may be larger, for example, in the short end of the bucket (along the maturity dimension) rather than at its long end. Along the same lines of the reasoning presented for the single risk factor case, it would be desirable to know the behaviour of the loss $l(\zeta)$ for each $\zeta \in Z$; however, mindful of the computational effort, the methodology requires the valuation of the loss only for those scenarios in Z_Θ:

$$Z_\Theta = \bigcup_{\beta \in \{0.8,1\}} \zeta_{\text{down}}(\beta) \;\cup \bigcup_{\beta \in \{0.8,1\}} \zeta_{\text{up}}(\beta) \,. \tag{47}$$

$FS_{D^*}(B)$, the extreme scenario of future shocks for the bucket B, is the scenario ζ in the set Z_Θ leading to the worst loss:

$$FS_{D^*}(B) = \underset{\zeta \in Z_\Theta}{\text{argmax}}\; l(\zeta) \,. \tag{48}$$

Analogously to the determination of the stress scenario risk measure for a single NMRF, for a bucket B:

$$SS_{10d}(B) = \begin{cases} K_{D^*}(B) \cdot l(FS_{D^*}(B)) & FS_{D^*}(B) \in \{\zeta_{\text{down}}(1); \zeta_{\text{up}}(1)\} \\ l(FS_{D^*}(B)) & FS_{D^*}(B) \in \{\zeta_{\text{down}}(0.8); \zeta_{\text{up}}(0.8)\} \end{cases} \tag{49}$$

where $K_{D^*}(B)$ is the non–linearity coefficient applicable at bucket level analogously to Eq. 26:

$$K_{D^*}(B) = \max\left(K_{\min}, \min\left(\tilde{K}_{D^*}(B), K_{\max}\right)\right) \,, \tag{50}$$

with $K_{\min} = 0.9$, $K_{\max} = 5$ and:

$$\tilde{K}_{D*}(B) = 1 + \frac{25}{2} \frac{l(0.8\, FS_{D*}(B)) - 2\, l(FS_{D*}(B)) + l(1.2\, FS_{D*}(B))}{l(FS_{D*}(B))} \left(\widehat{\phi_B} - 1\right), \tag{51}$$

where for simplicity and robustness the tail-parameter at bucket level $\widehat{\phi_B}$ is the median of the tail parameters $(\widehat{\phi_1}, \widehat{\phi_2}, ..., \widehat{\phi_{M_B}})$ of the M_B risk factors in bucket B. Also in this case, $SS_{10\mathrm{d}}(B)$ is floored to zero in the rare case that $l(FS_{D*}(B)) \leq 0$, and the maximum loss approach described in Subsection 5.2.4 can be used by supervisors to address specific cases.

7 Aggregated capital requirements for non-modelled risks

To finally determine the capital charge associated with non-modellable risk factors, $SS_{10\mathrm{d}}(j)$ is rescaled to reflect the NMRF's liquidity horizon LH_j. We obtain the final stress scenario risk measure $SS(j)$ by employing the FRTB square-root-of-time rule used for the liquidity horizon scaling for modellable risk factors:

$$SS(j) = SS_{10\mathrm{d}}(j) \sqrt{\frac{LH_j^{\mathrm{floored}}}{10}}, \tag{52}$$

where $LH_j^{\mathrm{floored}} = \max(LH_j, 20)$ is the liquidity horizon of the risk factor floored at 20 business days in accordance with paragraph MAR 33.16(1) of the FRTB standards. All risk factors within a bucket have the same liquidity horizon; thus, Eq. 52 is equivalently applicable at bucket level.

The capital requirements corresponding to all non-modellable risks are finally obtained by aggregating the stress scenario risk measure for each risk factor or bucket, as set out in paragraph MAR 33.17 of the FRTB:

$$SES = \sqrt{\sum_{i \in ICSR} SS(i)^2} + \sqrt{\sum_{j \in IER} SS(j)^2} + \sqrt{\left(\rho \sum_{k \in OR} SS(k)\right)^2 + (1-\rho^2) \sum_{k \in OR} SS(k)^2}, \tag{53}$$

where $\rho = 0.6$, *ICSR* and *IER* are respectively the sets of risk factors reflecting idiosyncratic credit spread risk and idiosyncratic equity risk only, and for which the bank is able to demonstrate that a zero correlation is appropriate. *OR* is the set of all other risk factors.

8 Summary and conclusions

In this paper, we design a methodology for capitalising the risk of non-modellable risk factors under the FRTB framework. We built it (i) to be applicable to any kind of risk factor by ensuring that its building blocks are not risk-factor dependent; (ii) to capture for a wide range of different cases with respect to the number of observations available for a given risk factor by generalising the concept of 10-business-day return and by introducing the asigma method under which an expected shortfall measure is approximated by rescaling a volatility measure of the returns; (iii) to target a level of capitalisation in line with the FRTB standards by setting the constants of the methodology consistently with the level of capital targeted in the standards; (iv) to capture the portfolio losses susceptible to a risk factor accurately while; (v) being efficient by evaluating only a few selected risk factor shocks and capturing non-linear behaviours of losses with only one additional portfolio loss evaluation.

Our methodology reduces the computational effort stemming from a naïve straightforward application of the FRTB standards, i.e. from a direct computation of the expected shortfall of the losses for each non-modellable risk factor, by a factor of around 50 ($\sim$ 250 business days per year compared to 5 selected shocks, including approximating non-linearity in the tails). Furthermore, it provides for a reasonably accurate ES calculation even where few data are available making the methodology universal, not only because it is applicable to any kind of risk factor, but also because it provides results in line with the FRTB standards even when few data

are available. While the methodology is applicable in most cases, we outline measures for supervisors to take in cases the methodology may not work well.

As a tool to analyse the statistical properties of risk factors, we use a family of SGT distributions with moments matched to a large set of historical risk factor data [EBA19, EBA20a, EBA20b]. Analysing the values taken by the relevant measures for those SGT distributions, we motivate the values of the methodology's parameters.

We study the sampling error in estimating the expected shortfall with different estimators by simulation of the family of SGT distributions, and design a simple uncertainty compensation factor to capture that uncertainty and reflect it in the capital requirements.

We finally show that the methodology can be naturally extended from the single risk factor level and be applied at the level of a segment of a risk factor curve or surface (the so-called 'regulatory buckets' described in the FRTB).

The methodology with minor differences has been successfully field tested by some of the largest banks in Europe on standardised and real trading portfolios [EBA19]. To our knowledge it is the first universal methodology with approximately controlled accuracy for the capitalisation of non-modellable risk factors publicly described in detail. More results will be available when banks use it to perform capital calculations under the FRTB internal model approach.

A Annex

This Annex defines the SGT distribution [The98] in the notation used in this paper and provides explitit expressions for value-at-risk and expected shortfall. For SGT distributions there are several parametrisations in literature. For our analyses using the R language [R C19] with the R package "sgt" [Dav15], we use the notation in the following independent parameters: μ, σ, λ, p, and q. μ and σ are the mean and standard deviation, λ with $-1 < \lambda < 1$ is the skewness parameter, $p > 0$ is the peakedness, and $q > 0$ the tail thickness parameter. The SGT distribution family encompasses many other distributions, cf. e.g. [HMN10], the most simple one being the standard normal distribution obtained for $\mu = 0$, $\sigma = 1$, $\lambda = 0$ (no skew), $p = 2$, and $q = \infty$. The same parameter values with a finite q lead to a Student's t distribution with $\nu = 2q$ degrees of freedom.

In this notation, the SGT distribution probability density is

$$f_{\mathrm{SGT}}(x;\mu,\sigma,\lambda,p,q) = \frac{p}{2v\sigma q^{\frac{1}{p}} B(\frac{1}{p},q)\left(\frac{|x-\mu+m|^p}{q(v\sigma)^p(\lambda\,\mathrm{sign}(x-\mu+m)+1)^p}+1\right)^{\frac{1}{p}+q}}\,, \tag{54}$$

and where for $pq > 1$, the helper variables m and v which are not parameters themselves, are defined as

$$m(\sigma,\lambda,p,q) := \frac{2v(\lambda,p,q)\sigma\lambda q^{\frac{1}{p}} B(\frac{2}{p},q-\frac{1}{p})}{B(\frac{1}{p},q)} = \tilde{m}(\lambda,p,q)v(\lambda,p,q)\sigma\,, \tag{55}$$

and

$$v(\lambda,p,q) := q^{-\frac{1}{p}}\left[(3\lambda^2+1)\frac{B(\frac{3}{p},q-\frac{2}{p})}{B(\frac{1}{p},q)} - 4\lambda^2\frac{B(\frac{2}{p},q-\frac{1}{p})^2}{B(\frac{1}{p},q)^2}\right]^{-\frac{1}{2}}. \tag{56}$$

B denotes the beta function. m is a location shift variable, such that we can express the mode as $mode = \mu - m$. With $m(\sigma,\lambda,p,q) = \tilde{m}(\lambda,p,q)v(\lambda,p,q)\sigma$ we separate the dependency on the rescaled standard deviation $v\sigma$, where v is a scaling variable for σ.

We first give the explicit expressions for the first four moments of the SGT distributions [TS16, MM17, The18b] (in different parametrizations) in our chosen parametrisation.

The i^{th} centralized moment $\mu_i := E[(R-E(R))^i]$ is finite for $pq > i$ only. Mean $\mu_1 = \mu$ and variance $\mu_2 = \sigma^2$ are distribution parameters, the third centralized moment is

$$\begin{aligned}\mu_3 = \frac{2q^{\frac{3}{p}}\lambda(v\sigma)^3}{B\left(\frac{1}{p},q\right)^3}\Bigg[&8\lambda^2 B\left(\frac{2}{p},q-\frac{1}{p}\right)^3 - 3(1+3\lambda^2)B\left(\frac{1}{p},q\right)B\left(\frac{2}{p},q-\frac{1}{p}\right)B\left(\frac{3}{p},q-\frac{2}{p}\right)\\ &+2\left(1+\lambda^2\right)B\left(\frac{1}{p},q\right)^2 B\left(\frac{4}{p},q-\frac{3}{p}\right)\Bigg]\,,\end{aligned} \tag{57}$$

and the forth centralized moment is

$$\begin{aligned}\mu_4 = \frac{q^{\frac{4}{p}}(v\sigma)^4}{B\left(\frac{1}{p},q\right)^4}\Bigg[&-48\lambda^4 B\left(\frac{2}{p},q-\frac{1}{p}\right)^4 + 24\lambda^2\left(1+3\lambda^2\right)B\left(\frac{1}{p},q\right)B\left(\frac{2}{p},q-\frac{1}{p}\right)^2 B\left(\frac{3}{p},q-\frac{2}{p}\right)\\ &-32\lambda^2\left(1+\lambda^2\right)B\left(\frac{1}{p},q\right)^2 B\left(\frac{2}{p},q-\frac{1}{p}\right)B\left(\frac{4}{p},q-\frac{3}{p}\right)\\ &+\left(1+10\lambda^2+5\lambda^4\right)B\left(\frac{1}{p},q\right)^3 B\left(\frac{5}{p},q-\frac{4}{p}\right)\Bigg]\,.\end{aligned} \tag{58}$$

The ES and VaR are key quantities in our analysis and can be expressed analytically for the SGT distribution by adding tail probability and shape dependent summands to the mode [The18a](in another parametrization). We give explicit formulae for the ES and VaR in our parametrization considering them useful for other studies.

The correspondence of the variables k_{Th}, n_{Th}, m_{Th}, ϕ_{Th}, and q_{Th} in [The18a] is as follows: $k_{\mathrm{Th}} = p$, $n_{\mathrm{Th}} = pq$, $m_{\mathrm{Th}} = mode$, $\phi_{\mathrm{Th}} = (v\sigma)/p^{\frac{1}{p}}$ and $q_{\mathrm{Th}} = \alpha = 2.5\%$ in our notation.

We define $t^*(\alpha)$ (Eq. (8) of [The18a]) which is controlled by the tail probability α:

$$t^*(\alpha;\lambda) := \frac{2\left|\alpha-\frac{1-\lambda}{2}\right|}{1+\mathrm{sign}\left(\alpha-\frac{1-\lambda}{2}\right)\lambda}\,, \tag{59}$$

Like in the R language, let $\text{pbeta}(x,a,b) = I_x(a,b)$ denote the incomplete beta function (definition 8.17.2 in [DLMF], sometimes also called incomplete beta function ratio [DJ66, DM92]), and $\text{qbeta}(x,a,b) = I_x^{-1}(a,b)$ denote the inverse of the incomplete beta function.

After setting

$$\tilde{W}(\alpha;\lambda,p,q) := \frac{(1-\lambda)^2}{2\alpha}\, q^{\frac{1}{p}}\, \frac{B\left(\frac{2}{p}, q-\frac{1}{p}\right)}{B\left(\frac{1}{p},q\right)} \left\{1 - \text{pbeta}\left[\text{qbeta}\left(t^*(\alpha;\lambda), \frac{1}{p}, q\right), \frac{2}{p}, q-\frac{1}{p}\right]\right\}, \tag{60}$$

Eq. 31 of [The18a] for the expected shortfall (same sign convention as our convention with a positive left tail ES of a distribution centred around zero) becomes

$$\text{ES}^{\text{SGT}}(\alpha) = -mode + \tilde{W}(\alpha;\lambda,p,q)\, v\sigma\,. \tag{61}$$

After dividing by $p^{\frac{1}{p}}$, Eq. 7 of [The18a] becomes:

$$\tilde{w}(\alpha;\lambda,p,q) = \text{sign}\left(\alpha - \frac{1-\lambda}{2}\right) q^{\frac{1}{p}} \left(\frac{\text{qbeta}(t^*(\alpha;\lambda), \frac{1}{p}, q)}{1-\text{qbeta}(t^*(\alpha;\lambda), \frac{1}{p}, q)}\right)^{\frac{1}{p}} \tag{62}$$

and the α-quantile in Eq. 6 of [The18a] is the negative value-at-risk (in our sign convention):

$$\text{VaR}^{\text{SGT}}(\alpha) = -mode - (1+\text{sign}(\tilde{w}(\alpha;\lambda,p,q))\lambda)\, \tilde{w}(\alpha;\lambda,p,q)\, v(\lambda,p,q)\sigma\,. \tag{63}$$

Hence, the ES and VaR are the mode plus the rescaled sigma times a pre-factor depending on the shape of the distribution and the tail probability. Recalling that $mode = \mu - m = \mu - \tilde{m}(\lambda,p,q)v(\lambda,p,q)\sigma$ is a linear function of $v(\lambda,p,q)\sigma$, too, we see that both risk measures are indeed a linear function of the standard deviation, as it should be for a location-scale family of distributions:

$$\text{ES}^{\text{SGT}}(\alpha;\mu,\sigma,\lambda,p,q) = -\mu + \tilde{m}v\sigma + \tilde{W}(\alpha;\lambda,p,q)\, v\sigma = -\mu + C_{\text{ES}}^{\text{SGT}}(\alpha;\lambda,p,q)\sigma\,, \tag{64}$$

and

$$\text{VaR}^{\text{SGT}}(\alpha;\mu,\sigma,\lambda,p,q) = -\mu + \tilde{m}v\sigma - (1+\text{sign}(\tilde{w}(\alpha;\lambda,p,q))\lambda)\, \tilde{w}(\alpha;\lambda,p,q)\, v\sigma = -\mu + C_{\text{VaR}}^{\text{SGT}}(\alpha;\lambda,p,q)\sigma\,. \tag{65}$$

The variables $C_{\text{ES}}^{\text{SGT}}$ and $C_{\text{VaR}}^{\text{SGT}}$ formally capture the terms depending on the shape of the normalized distribution and the tail probability α.

The analytical expressions for ES and VaR were checked against large sample simulated values, which were used in the investigation of the sampling distributions for the uncertainly compensation factor.

References

[AMLSG16] Pilar Abad, Sonia Muela, Carmen Lopez, and Miguel Sánchez-Granero. Evaluating the performance of the skewed distributions to forecast value-at-risk in the global financial crisis. *The Journal of Risk*, 18:1 – 28, May 2016.

[AT02] Carlo Acerbi and Dirk Tasche. On the coherence of expected shortfall. *Journal of Banking & Finance*, 26(7):1487–1503, Jul 2002.

[Bas19] Basel Committee on Banking Supervision. Minimum capital requirements for market risk. Standard d457, Bank for International Settlements, January 2019. https://www.bis.org/bcbs/publ/d457.pdf.

[Ben03] Joseph Bennish. A proof of Jensen's inequality. *Missouri J. Math. Sci.*, 15(1):33–35, 02 2003.

[BJPZ08] Vytaras Brazauskas, Bruce Jones, Madan Puri, and Ricardas Zitikis. Estimating conditional tail expectation with actuarial applications in view. *Journal of Statistical Planning and Inference*, 138:3590–3604, 11 2008.

[BS08] R. E. Baysal and J. Staum. Empirical likelihood for value-at-risk and expected shortfall. *Journal of Risk*, 11:3–32, 2008.

[CF38] E. A. Cornish and R. A. Fisher. Moments and cumulants in the specification of distributions. *Revue de l'Institut International de Statistique / Review of the International Statistical Institute*, 5(4):307–320, 1938.

[Dav15] Carter Davis. *sgt: Skewed Generalized T Distribution Tree*, 2015. R package version 2.0.

[DJ66] A. R. DiDonato and M. P. Jarnagin. A method for computing the incomplete beta function ratio. NWL report No. 1949, U. S. Naval Weapons Laboratory, Dahlgren, Virginia, October 1966.

[DLMF] *NIST Digital Library of Mathematical Functions.* http://dlmf.nist.gov/, Release 1.0.27 of 2020-06-15. F. W. J. Olver, A. B. Olde Daalhuis, D. W. Lozier, B. I. Schneider, R. F. Boisvert, C. W. Clark, B. R. Miller, B. V. Saunders, H. S. Cohl, and M. A. McClain, eds.

[DM92] Armido R. Didonato and Alfred H. Morris. Algorithm 708: Significant digit computation of the incomplete beta function ratios. *ACM Trans. Math. Softw.*, 18(3):360–373, September 1992.

[Dou09] Pierre Douillet. Sampling distribution of the variance. *Proceedings of the 2009 Winter Simulation Conference (WSC)*, pages 403–414, 2009.

[EBA19] EBA. EBA data collection on non-modellable risk factors. Data collection, European Banking Authority, Paris, France, June 2019. https://eba.europa.eu/eba-publishes-its-roadmap-for-the-new-market-and-counterparty-credit-risk-approaches-and-launches-consultation-on-technical-standards-on-the-ima-under.

[EBA20a] EBA. Draft Regulatory Technical Standards on the calculation of the stress scenario risk measure under Article 325bk(3) of Regulation (EU) No 575/2013. Consultation Paper EBA/CP/2020/10, European Banking Authority, Paris, France, June 2020. https://eba.europa.eu/calendar/consultation-paper-draft-regulatory-technical-standards-calculation-stress-scenario-risk.

[EBA20b] EBA. Final Draft Regulatory Technical Standards on the calculation of the stress scenario risk measure under Article 325bk(3) of Regulation (EU) No 575/2013 (Capital Requirements Regulation 2 - CRR2). Final Draft RTS EBA/RTS/2020/12, European Banking Authority, Paris, France, December 2020. https://www.eba.europa.eu/sites/default/documents/files/document_library/Publications/Draft Technical Standards/2020/RTS/961600/Final draft RTS on the calculation of stress scenario risk measure.pdf.

[EBA21] EBA. Supervisory benchmarking exercises. Regulatory activity overview, European Banking Authority, Paris, France, 2021. https://www.eba.europa.eu/regulation-and-policy/supervisory-benchmarking-exercises.

[Far93] Stanley J. Farlow. *Partial Differential Equations for Scientists and Engineers*. Dover Publications, 1993.

[FC60] Ronald A. Fisher and E. A. Cornish. The percentile points of distributions having known cumulants. *Technometrics*, 2(2):209–225, 1960.

[GT71] John Gurland and Ram C. Tripathi. A simple approximation for unbiased estimation of the standard deviation. *The American Statistician*, 25(4):30–32, 1971. Equation 6.

[HMN10] Christian Hansen, James B. McDonald, and Whitney K. Newey. Instrumental variables estimation with flexible distributions. *Journal of Business and Economic Statistics*, 28(1):13–25, 2010.

[Hür02] Werner Hürlimann. Analytical bounds for two value-at-risk functionals. *ASTIN Bulletin*, 32(2):235–265, 2002. Theorem 3.1.

[Int20] Intesa Sanpaolo, Financial and market risk department. Response to EBA Consultation on Regulatory Technical Standards on the calculation of the stress scenario risk measure for NMRF. Public consultation response letter, Intesa Sanpaolo S.p.A., Turin, Italy, September 2020. https://www.eba.europa.eu/node/102208/submission/96851.

[Jen06] J. L. W. V. Jensen. Sur les fonctions convexes et les inégalités entre les valeurs moyennes. *Acta Math.*, 30:175–193, 1906.

[JG98] D. N. Joanes and C. A. Gill. Comparing measures of sample skewness and kurtosis. *Journal of the Royal Statistical Society. Series D (The Statistician)*, 47(1):183–189, 1998.

[KM13] Sean C. Kerman and James B. McDonald. Skewness–kurtosis bounds for the skewed generalized t and related distributions. *Statistics & Probability Letters*, 83(9):2129 – 2134, 2013.

[KMv00] Chris A.J. Klaassen, Philip J. Mokveld, and Bert van Es. Squared skewness minus kurtosis bounded by 186/125 for unimodal distributions. *Statistics & Probability Letters*, 50(2):131 – 135, 2000.

[LN20] Riu Li and Saralees Nadarajah. A review of Student's t distribution and its generalizations. *Empirical Economics*, 58:1461–1490, March 2020.

[Mai18] Didier Maillard. A user's guide to the Cornish Fisher expansion. *SSRN*, May 2018. Available at SSRN: https://ssrn.com/abstract=1997178.

[MBP17] Adolfo Montoro, Tim Becker, and Lars Popken. Identification and capitalisation of non-modellable risk factors. risk.net, January 2017.

[MH05] B. John Manistre and G. Hancock. Variance of the CTE estimator. *North American Actuarial Journal*, 9:129 – 156, 2005.

[MM17] James B. McDonald and Richard A. Michelfelder. Partially adaptive and robust estimation of asset models: Accommodating skewness and kurtosis in returns. *Journal of Mathematical Finance*, 7:219–237, 2017.

[NZC14] Saralees Nadarajah, Bo Zhang, and Stephen Chan. Estimation methods for expected shortfall. *Quantitative Finance*, 14(2):271–291, 2014.

[PC13] European Parliament and Council. Regulation (EU) No 575/2013 of the European Parliament and of the Council of 26 June 2013 on prudential requirements for credit institutions and investment firms and amending Regulation (EU) No 648/2012 (Capital Requirements Regulation) as amended. *Official Journal of the European Union*, L 176, June 2013. http://data.europa.eu/eli/reg/2013/575/oj.

[PC19] European Parliament and Council. Regulation (EU) 2019/876 of the European Parliament and of the Council of 20 May 2019 amending Regulation (EU) No 575/2013 as regards the leverage ratio, the net stable funding ratio, requirements for own funds and eligible liabilities, counterparty credit risk, market risk, exposures to central counterparties, exposures to collective investment undertakings, large exposures, reporting and disclosure requirements, and Regulation (EU) No 648/2012 (Capital Requirements Regulation 2) as amended. *Official Journal of the European Union*, L 150, May 2019. http://data.europa.eu/eli/reg/2019/876/oj.

[R C19] R Core Team. *R: A Language and Environment for Statistical Computing*. R Foundation for Statistical Computing, Vienna, Austria, 2019.

[The98] Panayiotis Theodossiou. Financial data and the skewed generalized t distribution. *Management Science*, 44:1650–1661, Dec 1998.

[The18a] Panayiotis Theodossiou. Risk measures for investment values and returns based on skewed-heavy tailed distributions: Analytical derivations and comparison. *SSRN Electronic Journal*, May 2018. https://ssrn.com/abstract=3194196.

[The18b] Panayiotis Theodossiou. Skewed generalized t and nested probability distributions: Specification and moments. *SSRN Electronic Journal*, May 2018. https://ssrn.com/abstract=3178548.

[TS16] Panayiotis Theodossiou and Christos S. Savva. Skewness and the relation between risk and return. *Management Science*, 62(6):1598–1609, 2016.

ACKNOWLEDGEMENTS

The methodology in the paper has benefited from discussions with several colleagues and different stakeholders. In particular, we would like to thank Svenja Israel, Philip Rau and Despo Malikkidou, all members of the EBA sub-group on Market Risk and its chair Stéphane Boivin, for their precious work in building up the methodology, as well as Lars Jul Overby and an anonymous referee for their comments. Any remaining errors are our own.

The opinions expressed are those of the authors and are not the responsibility of the institutions.

Martin Aichele:
Team Lead Banking Supervision, Directorate General Onsite & Internal Model Inspections, European Central Bank

Marco Giovanni Crotti:
Policy Expert, Directorate Prudential Regulation and Supervisory Policy, European Banking Authority

Benedikt Rehle*:
Parliamentary Assistant, European Parliament
(*) At the time of developing the methodology described in this paper, Mr. Rehle served as on-site inspector at Deutsche Bundesbank and was a representative at the EBA sub-group on Market Risk

EUROPEAN BANKING AUTHORITY

20 avenue André Prothin CS 30154
92927 Paris La Défense CEDEX, France

Tel. +33 1 86 52 70 00
E-mail: info@eba.europa.eu

https://eba.europa.eu/

ISBN 978-92-9245-747-1 doi:10.2853/859367
ISSN 2599-7831 DZ-AH-21-004-EN-N